Dissertation
submitted to the
Combined Faculties for Natural Sciences and for Mathematics
of the Ruperto-Carola University of Heidelberg, Germany
for the degree of
Doctor of Natural Sciences

presented by
Harsha Garadi Suresh, MSc- Molecular Biosciences
born in Bangalore, India
Oral examination on 18.12.2014

Fatty acid synthetase reversibly sequesters into storage granules upon nutrient limitation

Referees: Prof. Dr. Bernd Bukau
Dr. Brian Luke

I hereby declare that I have written the submitted dissertation myself and in this process have used no other sources or materials than those explicitly indicated.
The work was carried out at the Zentrum für Molekulare Biologie der Universität Heidelberg (ZMBH) in the group of Prof. Dr. Bernd Bukau.

Heidelberg, September 2014 Harsha Garadi Suresh

To my family

Contents

Abstract

It is increasingly apparent that protein aggregation is an organized event orchestrated by a variety of cellular factors, resulting in sequestration of proteins spatially, into distinct compartments. Some sequestrations occur in consequence of proteotoxic stress and sequester misfolded proteins into inclusions while others sequester under conditions of nutritional stress.

Recently, numerous cellular factors have been observed to form inclusions under conditions of starvation. In some cases, co-sequestration of functionally related proteins has also been observed. While some of these sequestrations have been proposed to represent either storage assemblies or enzyme clusters for increased localized activity, other reports claim them to be aggregates of misfolded proteins. Owing to such opposing views of starvation induced formation of inclusions, the precise nature, physiological role and their relationship to classical protein aggregates remains to be clarified.

Fatty acid synthetase (FAS), a key metabolic enzyme, being prone to sequestration under conditions of both proteotoxic and metabolic stress, provides an ideal model substrate for a study intending to clarify the above-mentioned controversy and thus is the model of choice for my study.

I find that both subunits of the heterodimeric FAS accumulates into one or more foci per cell depending on the starvation conditions. Unlike the classical protein aggregates, FAS foci retain enzymatic activity, their formation is Hsp42 independent and they do not co-localise with the AAA+ protein disaggregase, Hsp104. Moreover, addition of glucose alone triggers their resolubilisation in an Hsp104 independent manner, indicating foci formation to be reversible. While misfolded protein aggregates tend to mix, FAS is sequestered in the cytosol at a site distinct from other known sequestrations. Taken together, FAS foci formed during starvation are reversible active protein assemblies and are distinct from misfolded protein aggregates.

One could envision two possible physiological roles for FAS sequestration. FAS sequestration 1) is an event favoring localized synthesis of fatty acids and phospholipids. 2) represents storage assemblies.

While other enzymes of phospholipid and ergosterol biosynthesis also sequester upon starvation, they do not co-cluster with FAS. Thus, the phenomenon of co-clustering of functionally related enzymes is not conserved for lipid biosynthetic enzymes under conditions tested. This negates the first possibility of FAS sequestration to represent enzyme assemblies for efficient synthesis of phospholipids. This is consistent with the observation that prevention of FAS sequestration by genetic manipulation did

not affect cellular viability under starvation conditions. Thus, it is likely that FAS sequestration serves to spatially limit FAS availability, perhaps, in an attempt to conserve the cellular pool of its substrate, Acetyl-coA, a key metabolite in central metabolism. The conserved Acetyl-coA pool could in turn be utilized for other cellular processes that are vital for cellular adaptation to starvation.

The precise trigger for FAS sequestration remains unknown. Mutants altering the nutrient sensing and the lipid transport (secretory pathway) increased the rate of FAS sequestration indicating the metabolic status is likely to trigger FAS sequestration. I however, do not observe any obvious correlation between changes in lipid profile during starvation and FAS sequestration.

My study also extends the known sequestration of cytosolic proteins to entire organelles. Mitochondria and ER undergo reversible spatial reorganisation during starvation. These organellar changes correlate well with the alterations in lipid profiles indicating that the lipid flux between the two organelles could be affected during starvation. The physiological role of the observed changes remains to be determined.

Taken together, this study distinguishes starvation-induced granules from misfolded protein aggregates and sheds light on the nature and possible physiological role of starvation induced sequestrations and thereby clarifying the existing controversy on starvation induced inclusions. Moreover, this study extends the known localization changes from cytosolic enzymes to entire organelles thereby extending our knowledge on metabolism driven organellar dynamics.

Zusammenfassung

Proteinaggregation ist ein organisierter Prozess, welcher durch eine Vielzahl zellulärer Faktoren kontrolliert wird und zur Ablagerung von Proteinen in spezifischen Einschlußkörpern führt. Proteinablagerungen können durch missgefaltete Proteine während proteotoxischem Stress oder unter Bedingungen von Nährstofflimitation, metabolischem Stress, gebildet werden.

Verschiedene zelluläre Faktoren bilden Einschlußkörper bei Verknappung von Nährstoffen. In einigen Fällen werden Partnerproteine, welche gemeinsame zelluläre Funktionen besitzen, zusammen abgelagert. Die Rolle dieser Ablagerungen wird kontrovers diskutiert. Sie stellen entweder ein Speicherdepot für nicht benötigte Proteine dar, oder erhöhen die enzymatischen Aktivitäten der abgelagerten Proteine. Andere Studien charakterisieren sie als Aggregate von missgefalteten Proteinspezies. Die physiologische Bedeutung der Einschlußkörper und ihre Beziehung zu klassischen Proteinaggregaten bedarf daher der genaueren Analyse.

Fettsäuresynthetase (FAS), ein Schlüsselenzym im Lipidstoffwechsel, bildet Einschlußkörper unter proteotoxischem und metabolischem Stress und wurde daher von mir als Modellsubstrat zur vergleichenden Charakterisierung der Proteinablagerungen verwendet.

Ich konnte zeigen, dass beide Untereinheiten von heterodimerem FAS in ein oder mehrere Einschlußkörper abgelagert werden, abhängig von den Bedingungen der Nährstofflimitation. Im Gegensatz zu klassischen Proteinaggregaten zeigen diese FAS-Einschlußkörper enzymatische Aktivität. FAS-Einschlußkörper werden unabhängig von Hsp42 gebildet und sie kolokalisieren nicht mit der AAA+ Disaggregase Hsp104. Die Bildung der Einschlußkörper ist reversibel und kann durch Glukosezugabe unabhängig von Hsp104 revertiert werden. Während die Aggregation von missgefalteten Proteine zu gemischten Einschlußkörpern führt, zeigt FAS keine Kolokalisation mit anderen bekannten Proteinablagerungen, welche unter metabolischem Stress gebildet werden. Zusammen zeigen diese Befunde, das unter Nährstofflimitation gebildete FAS-Ablagerungen dynamisch sind und sich grundlegend von klassischen Proteinaggregaten unterscheiden.

Enzyme, welche in Phospholipid- und Ergosterol-Biosynthese involviert sind, bilden ebenfalls Ablagerungen während metabolischem Stress, kolokalisieren jedoch nicht mit FAS-Einschlußkörpern. Die gemeinsame Ablagerung von funktionell verbundenen Enzymen findet nicht statt, ein Befund der die Funktion der Einschlußkörper als Proteinspeicher unterstützt. Entsprechend hat das Unterbinden der Ausbildung von FAS-Einschlußkörpern keinen Effekt auf das Überleben von Zellen unter Nährstofflimitation. FAS-Einschlußkörper limitieren möglicherweise die lokale Verfügbarkeit

des Enzyms und verhindern dadurch die Umsetzung des Substrats Acetyl-CoA, welches ein zelluläres Schlüsselmetabolit darstellt.

Der zelluläre Auslöser der FAS-Ablagerung bleibt unbekannt. Mutanten, welche zu Veränderungen im Lipidtransport oder im Messen des Nährstoffangebots führen, zeigen eine erhöhte Rate der FAS Einschlußkörperbildung. Eine Korrelation zwischen Änderungen der Lipidzusammensetzung während metabolischem Stress und FAS-Ablagerung konnten jedoch nicht beobachtet werden.

Meine Arbeit erweitert die zuvor beschriebene lokale Ablagerung von Proteine auf gesamte Zellorganellen. Mitochondrien und ER zeigen während Nährstofflimitation eine reversible räumliche Umorganisation. Diese Strukturänderungen korrelieren mit Änderungen im Lipidprofil und weisen auf einen geänderten Lipidaustausch zwischen Mitochondrien und ER hin. Die physiologische Bedeutung der Reorganisation der Zellorganellen muss nachfolgend bestimmt werden.

Zusammenfassend zeigt diese Arbeit fundamentale Unterschiede zwischen Proteinablagerungen, welche unter metabolischem und proteotoxischen Stressbedingungen gebildet werden, auf. Sie gibt Aufschluß über die mögliche Rolle der unter Nährstofflimitation gebildeten Einschlußkörper und trägt somit zur Klärung existierender, widersprüchlicher Modelle bei. Weiterhin erweitert diese Arbeit das Spektrum der beschriebenen zellulären Restrukturierung unter metabolischem Stress von einzelnen Proteinen zu gesamten Zellorganellen.

List of Figures

List of Tables

1 Introduction

1.1 Protein aggregation

Proteotoxic stress can overwhelm the protein quality control system resulting in the accumulation of partially folded or misfolded proteins. Misfolded proteins often expose hydrophobic amino acid residues or regions of unstructured polypeptide backbone, which would otherwise be buried in the native structure, leading to non-native intra and intermolecular interactions that result in the formation of protein aggregates[1, 2, 3]. Typically, such non-native hydrophobic interactions result in the formation of amorphous aggregates. Alternatively, aggregation can lead to the formation of highly ordered, fibrillar aggregates called amyloid, in which β-strands run perpendicular to the long fibril axis (cross-β-structure). The formation of amyloid fibrils may have severe consequences on cellular physiology [4, 5, 6, 7].

1.1.1 Sequestration of misfolded proteins into distinct quality control compartments

Under proteotoxic stress, misfolded proteins typically harbouring hydrophobic residues accumulate and interact unspecifically with other cellular factors hindering their folding status and function. Given that many of these cellular factors are crucial for cellular viability, loss of their functional status could therefore be toxic making it imperative for cells to spatially regulate the accumulation of misfolded proteins. Indeed, in yeast, upon elevated temperature, overexpression of a constitutively misfolding substrate such as mcherry-VHL or GFP-Ubc9ts leads to accumulation of these substrates into distinct sequestrations [8](Figure 1.1). One that is in close proximity to the vacuole is termed IPOD (Insoluble Protein deposit) while the other accumulating adjacent to nucleus is termed Juxta-nuclear quality control compartment (JUNQ) [8].

Ubiquitination of misfolded proteins was reported to be both essential and sufficient for their targeting to JUNQ [8]. FLIP experiments indicate JUNQ to represent dynamic structures co-localising with Cim5-GFP and Hsp104-GFP, markers for 20S proteasome and the AAA+ disaggregase respectively. JUNQ is therefore believed to be a compartment for protein disaggregation and degradation. Terminally misfolded amyloid aggregates such as prion proteins (Ure2-GFP, RNQ1-GFP) and HttQ103-GFP were found to be accumulating at IPOD. mcherry-Atg8, a marker

for pre-autophagosomal structure (PAS) co-localises with IPOD markers indicating a possible involvement of autophagy in degradation of protein aggregates. Hsp104-GFP was observed to be co-localising with IPOD markers as well [8]. Both these compartments (JUNQ and IPOD) are asymmetrically segregated during cell division and this principle is believed to be one of the possible contributors of cellular ageing and rejuvenation [9].

A more careful time course study indicated accumulation of misfolded proteins into multiple aggregates termed peripheral aggregates [10]. The small heat shock protein Hsp42 is required for the formation of peripheral aggregates (Figure 1.1) as its absence results in the accumulation of misfolded reporters primarily at the JUNQ. The observed role of Hsp42 is further supported by the fact that Hsp42 exclusively co-localises with peripheral aggregates but not to JUNQ [10]. Another recent report identified accumulation of misfolded proteins into multiple Endoplasmic reticulum (ER) associated punctae upon heat shock termed as Q bodies, which then fuse with each other in an energy dependent but cytoskeleton independent manner [11]. Like peripheral aggregates, Hsp42 was also found to be essential for the formation of Q-bodies [11].

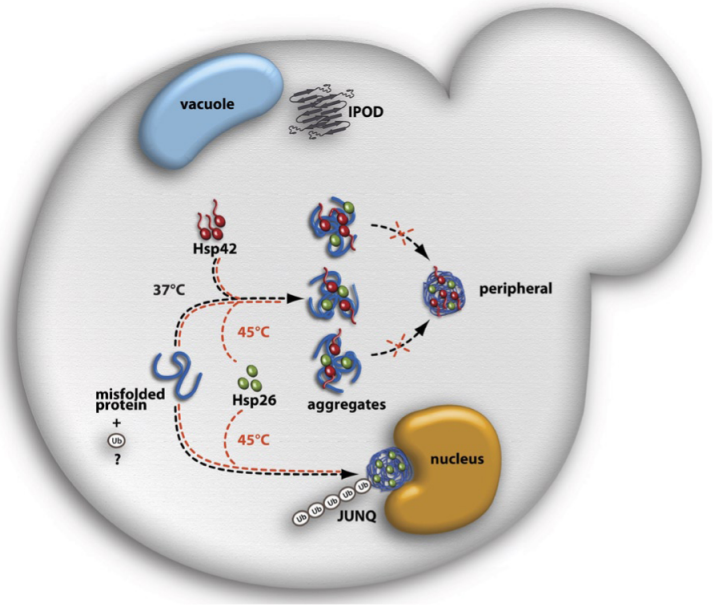

Figure 1.1: Spatial sequestration of misfolded proteins in yeast.

Heat shock induced misfolded proteins sequester into multiple peripheral aggregates (Q-bodies) [10, 11]. The small heat shock protein Hsp42 is required for Q-bodies formation and exclusively associates with peripheral protein aggregates but is absent from juxtanuclear aggregates (JUNQ) [10]. These Q-bodies coalese with each other [11]. Hsp26, another sHsp, associates with peripheral and juxtanuclear aggregates only during severe heat stress (45°C). Hsp42 does not associate with IPOD compartment harboring amyloidogenic proteins close to the vacuole [10, 11]. Ubiquitination (Ub) might serve as a sorting signal for juxtanuclear aggregates. Adapted from[10].

Recently, another cellular factor termed Btn2 was shown to be essential for the accumulation of misfolded protein reporters at the JUNQ [12]. Summarized, sequestration of misfolded proteins is an organized event orchestrated by the interplay of numerous cellular factors.

1.1.1.1 Role of sHsps in aggregate organization and disaggregation

sHsps are lower molecular weight ATP independent chaperones that aid in sorting of misfolded proteins and their disaggregation. The main hallmark of sHsps is the α-crystallin domain. Despite this conserved structural domain, sHsps vary widely in their N- and C-terminal extensions contributing to their substrate specificity.

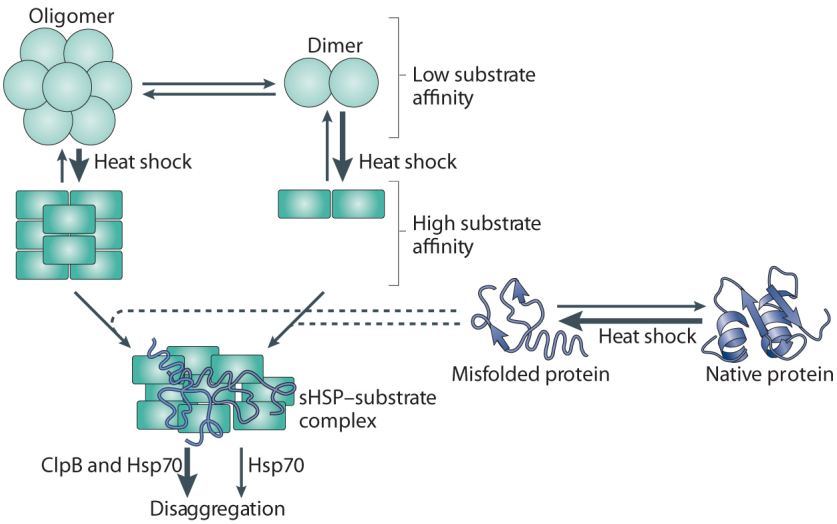

Figure 1.2: Activation and mode of action of sHsps in protein disaggregation. Small heat shock proteins (sHSPs) exist as oligomers that are in equilibrium with their exchanging subunits. They exist either in low or high substrate affinity states. Upon heat shock, the equilibrium shifts towards the high affinity state that form a stable complex with heat labile misfolded proteins. The sHsps-misfolded protein complex aids in sorting of misfolded proteins to quality control compartments where they can facilitate their re-solubilization together with the Hsp70-Hsp104 bichaperone system. Adapted from[9].

There are two known representatives of sHsps in yeast, namely, Hsp26 and Hsp42. Hsp26 is a 24mer, inactive at normal growth temperature but gets activated at elevated temperatures via intermolecular rearrangements (Figure 1.2) Such a temperature-dependent activation is not required for Hsp42. sHsps bind unfolded proteins preventing temperature-induced uncontrolled aggregation as well as sequestering them to form aggregates. Co-aggregation of sHsps enhances the accessibility for the Hsp70-Hsp104-bichaperone system toward protein aggregates and thereby increasing the efficiency of protein disaggregation (Figure 1.2). Recently, Hsp42 was

implicated in sorting of misfolded proteins into quality control compartments [10] as well as in the sequestration of Hos2 and Yca1 in stationary phase cells [13].

1.1.1.2 Disaggregation of protein aggregates by Ssa-Hsp104 bichaperone system

Ssa is a Hsp70 chaperone that is mainly discussed for its role in post-translational protein folding. It has however been implicated in co-translation protein folding as well [2, 14]. Four genes Ssa1 to Ssa4 encode for this Hsp70 chaperone [15]. While SSA3 and SSA4 are stress-inducible genes, SSA1 and SSA2 are constitutively expressed, although protein levels of Ssa2 are clearly above those of Ssa1 which is further induced under stress.

Hsp70s harbors an ATPase domain and a substrate-binding domain. The ATPase activity is stimulated by another class of factors called J-domain proteins (Hsp40s). In the ATP bound state, polypeptides bind to the substrate-binding domain of Hsp70 with low affinity. Upon stimulation of ATPase activity of Hsp70 by an Hsp40, there is an intra-molecular allosteric communication leading to tight binding of polypeptides in the substrate binding domain of Hsp70. Subsequently, a family of nucleotide exchange factors (NEFs) stimulate the nucleotide exchange leading to loading of ATP and the release of folded substrate (Figure 1.3) The substrate might have to undergo repeated cycles of action of Hsp70 and/or be transferred to downstream acting chaperone systems to achieve its native state [16]. Its functional system, in addition to Hsp70 consists of Hsp40 proteins such as Ydj1 or Sis1 among others and Sse1 or Fes1 (NEFs).

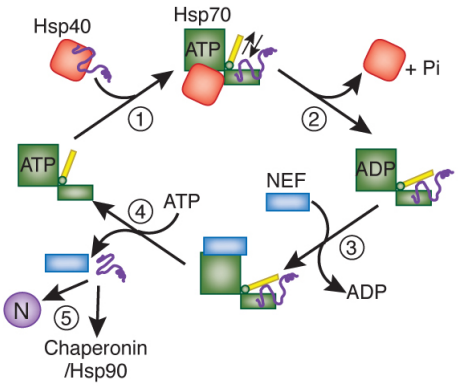

Figure 1.3: Hsp70 functional cycle.
Hsp70 functional cycle involves the following steps: (1) Hsp40-mediated delivery of substrate to ATP-bound Hsp70. (2) Hydrolysis of ATP to ADP mediated by Hsp40 results in closing of the α-helical lid and tight binding of substrate by Hsp70. Subsequently, Hsp40 dissociates from Hsp70. (3) NEF catalyzes exchange of ADP for ATP. (4) Opening of the α-helical lid, induced by ATP binding, results in substrate release. (5) Released substrate either folds to native state (N), is transferred to downstream chaperones or rebinds to Hsp70. Adapted from [16].

Hsp104 is a homohexameric AAA+ disaggregase belonging to the Hsp100 chaperone

family. Each monomer of Hsp104 contains two ATPase domains (AAA-1 and AAA-2), an N-terminal domain and a middle domain, which is inserted into AAA-1 [17, 9]. ATP hydrolysis driven structural rearrangements within the hexameric ring of Hsp104 mediates cycles of substrate binding and release through its central pore leading to disaggregation of proteins (Figure 1.4) [18, 19]. Apart from targeting Hsp104 to surface of protein aggregates, Ssa also aid in folding of substrates threaded through the central pore of Hsp104 and thus acting both upstream and downstream of Hsp104 activity [17, 9].

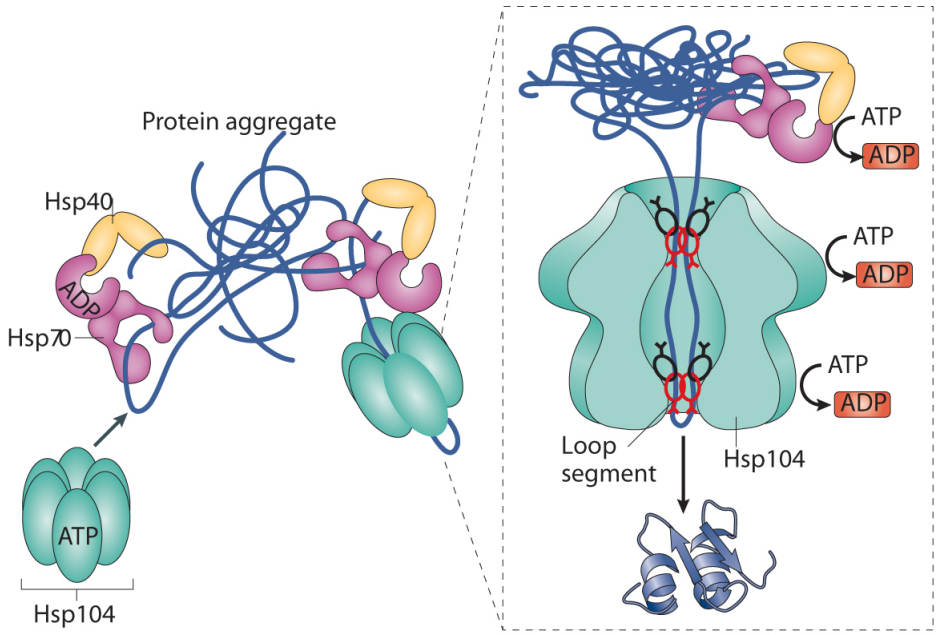

Figure 1.4: Hsp70-Hsp104 bichaperone system mediated protein disaggregation.
Hsp70 is targeted to hydrophobic patches in the aggregate by Hsp40, which also stimulates ATP hydrolysis in the NBD of Hsp70 and mediates tight peptide binding. Hsp104 hexamer pulls the peptide into the central pore, where it is threaded and unfolded by the pulling force of hydrophobic residues. Adapted from [9].

The middle domain of Hsp104 functions as a key regulatory switch that regulates the activity of Hsp104. Middle domain (M) with two wings, motif 1 and motif 2, is essential to disaggregation. Motif 2 docks intra-molecularly to AAA-1 to regulate Hsp104 unfolding power, and motif 1 contacts a neighboring AAA-1 domain. Mutations that stabilize motif 2 docking repress Hsp104, whereas destabilization leads to de-repressed Hsp104 activity with greater unfolding power that is toxic in vivo. Moreover, interaction of Hsp70 Ssa with M domain also contributes to the activation of Hsp104 [20, 21].

Apart from their action on amorphous heat denatured aggregates, Ssa-Hsp104-bichaperone system is also implicated in prion (amyloids) fragmentation and propagation [22].

1.2 Coordination of protein disaggregation and translational reinitiation upon severe heat stress

A recent systematic study demonstrated that, upon severe heat shock, heat stress granules (heat-SGs) contain mRNA, translation machinery components (excluding ribosomes), and molecular chaperones (Ssa and Hsp104)[23]. Additionally, heat-SGs coassemble with aggregates of misfolded, heat-labile proteins. Components in these mixed assemblies exhibit distinct molecular motilities that reflect differential trapping. Moreover, restoration of translation activity during heat stress recovery is intimately linked to disaggregation of damaged proteins present in the mixed assemblies and requires Hsp104 and Hsp70 activity. Thus, chaperone driven heat-SG disassembly directly coordinates the timing of translation reinitiation with protein folding capacity during cellular quality control surveillance, enabling efficient protein homeostasis (Figure 1.5) [23].

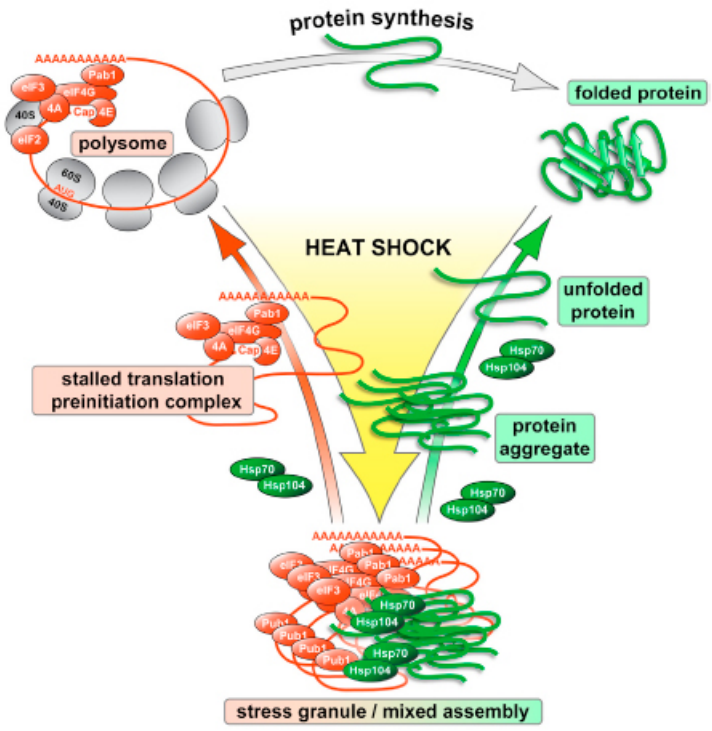

Figure 1.5: Model of protein homeostasis maintained through sequestration of translation machinery in protein aggregates.
Heat-labile proteins aggregate after a modest rise in temperature and provide scaffolds for assembly of stalled translation preinitiation complexes at higher temperatures. This leads to the formation of mixed assemblies of protein aggregates and heat-SGs. Chaperone induction and return to lower temperature reduces the load of aggregated proteins, which in turn liberates preinitiation complexes from mixed assemblies and enables translation reinitiation. Adapted from [23].

Unpublished work from our laboratory also find chaperones involved in co-translational protein folding and targeting, namely Ssb and Nascent chain associated complex (NAC) to coassemble with heat SGs.

Nascent chain associate complex (NAC) is one of the ribosome associated chaperone complex consisting of α and β subunits. The α subunit is constituted by Egd2p while the β subunit is represented by either Egd1p or Btt1p. The NAC complex associates with the ribosome through its β subunit while both α and β subunits are known to interact with nascent polypeptides (Figure 1.6). However, the precise role of NAC in protein folding remains enigmatic. In recent times, NAC has been proposed to have roles in co-translational protein targeting as well as biogenesis of ribosomes [24, 25, 26].

Ssb is an Hsp70 chaperone that associates directly with the ribosome (Figure 1.6). There are two isoforms of Ssb- Ssb1 and Ssb2, which only differ by 4 amino acids in their composition[27].

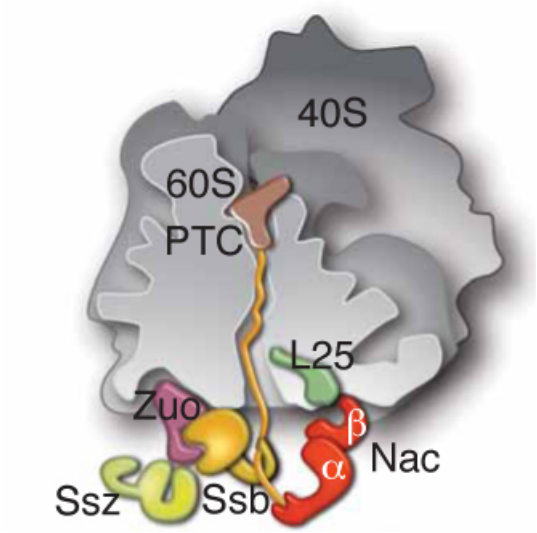

Figure 1.6: Co-translational protein folding in *S.cerevisiae*.

The ribosome bound chaperone systems (Ssb-RAC system and NAC) bind to nascent polypeptides and aid in their folding in association with other downstream cellular chaperone systems (Ssa, Hsp90). Alternatively, they aid in targeting of nascent proteins by preventing their premature folding Adapted from [27].

The Ribosome associated complex (RAC) consisting of J-domain protein Zuo1p and Ssz1p, which together stimulate the ATPase activity of Ssb at the ribosome [28, 29, 30, 31, 32, 33, 34] while Snl1, Fes1 and Sse1 can individually act as NEFs of Ssb [35, 36, 37, 38].

Recent evidence suggests that Ssb associates with a subset of newly synthesized polypeptides whose intrinsic properties and slow translational rates hinder the co-translational protein folding [32]. Deletion of any single component of the triad (Ssb, Zuo1 or Ssz1) causes similar cellular defects, including cold and salt sensitivity,

slow growth and hypersensitivity toward aminoglycosides, indicating a functional interplay [34, 39, 40]. Ssb directly associates with ribosomes and has been reported to bind to a large fraction of nascent chains and to protect them from off pathways that eventually lead to misfolding and ubiquitination [34, 39, 41, 42, 43]. Other than its role in co-translational protein folding, Ssb is involved in ribosome biogenesis [25, 26] and regulation of Snf1 mediated glucose sensing [44].

While both Ssb and NAC perform various vital functions in the cell, none of their above-mentioned functions of these ribosome-associated chaperones explain their coassembly with heat SGs. This opens up possibilities for their involvement in other novel cellular functions that are not appreciated so far.

1.3 Elimination of misfolded proteins and protein aggregates

Some proteins that are terminally aggregated or damaged (such as protein carbonylation) cannot be disaggregated efficiently by chaperone machineries of the cell. Additionally, under conditions of severe proteotoxic stress, chaperone machineries are overwhelmed and thereby necessitating alternate pathways for clearing misfolded proteins and their aggregates [45]. In yeast, there are two pathways that aid in degradation of misfolded and aggregated proteins. They are:

1) Ubiquitin-Proteasome system

Chains of a small protein termed ubiquitin are covalently attached to irreversibly damaged, misfolded and short-lived proteins. This is achieved by a concerted action of a network of E1 ubiquitin activating enzymes, E2 ubiquitin conjugating enzymes and E3 ubiquitin ligases. Labeling proteins by polyubiquitin chains targets them to degradation by a large and highly selective proteolytic system known as the 26S proteasome [45].

The 26S proteasome consists of a proteolytic barrel-shaped 20S core particle, which is capped on both ends with a regulatory 19S subunit. The regulatory subunit of the proteasome contains ubiquitin receptors that recognize and bind to the polyubiquitin chains of target proteins. After the substrate binding, the bulky polyubiquitin chains are removed through isopeptidase action of the 19S subunit. The action of AAA+ rings of the regulatory subunit aids in subsequent substrate unfolding and translocation into the proteolytic cavity of the proteasome where the substrates are broken down into short polypeptides (8-10 residues in length) [45].

2) Autophagy

While proteasome degrades most misfolded proteins, mutants defective in ubiquitin mediated degradation or upon inhibition/overwhelming of proteasomal activity, misfolded proteins are degraded via an alternate path termed autophagy [46]. Autophagy is a key cellular process that involves bulk engulfment of cellular components by double membrane structures leading to the formation of autophagosomes. Autophagosomes in turn fuse with the vacuole leading to the degradation of its contents [47]. While autophagy was long considered to be a bulk unspecific degradation of cellular contents, mechanisms for selective turnover of organelles and aggregates have been recently elucidated [47, 9].

Recently, it was reported that Rsp5 mediated ubiquitination of huntington derived polyQ and heat-labile proteins are degraded via autophagy in starved yeast cells [48]. A CUET family ubiquitin binding protein Cue5 facilitates their degradation by interacting with both ubiquitinated substrates and Atg8, a key component of autophagosomes (Figure 1.7) [48].

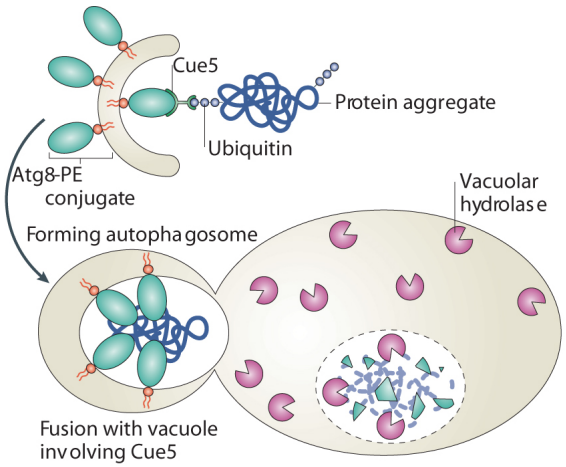

Figure 1.7: Cue5 mediated autophagic degradation of heat-labile and huntington derived polyQ ubiquitinated aggregated proteins.
Ubiquitylation of protein aggregates is a signal that triggers binding of the adaptor protein Cue5, which also binds Atg8 conjugated with lipids in the double membrane of the forming autophagosome. This allows cargo, in this case, a protein aggregate to be included in the forming autophagosome, which subsequently fuses with vacuole to release its inner-membrane vesicle with included aggregate for hydrolytic degradation. PE, phosphatidylethanolamine. Adapted from [9].

1.4 Metabolic stress induced sequestration of proteins

Recently, it is becoming clear that metabolic stress such as nutrient limitation (stationary phase) also induces sequestration of proteins and the phenomenon seems to be conserved from yeast to humans [49, 50, 51, 52, 53]. In yeast, carbon starvation leads to reorganization of the actin cytoskeleton and the formation of actin bodies [54]. Proteasomes relocalize from the nucleus to the cytosol to form proteasome storage granules [51]. A global screen for yeast proteins forming insoluble deposits upon starvation identified 180 proteins, many of them being metabolic enzymes [53]. Protein sequestrations formed during stationary phase are often reversible and are solubilized upon addition of specific metabolites [53, 52, 55, 50], proposing the foci to be storage assemblies. Co-sequestration of functionally related proteins has been reported such as for Ura7/Ura8 that are involved in CTP biosynthesis in yeast or enzymes involved in purine biosynthesis in mammalian cells [50, 52]. It was postulated that co-clustering of enzymes during metabolic stress aids in enhanced substrate channeling and more efficient biosynthetic activity.

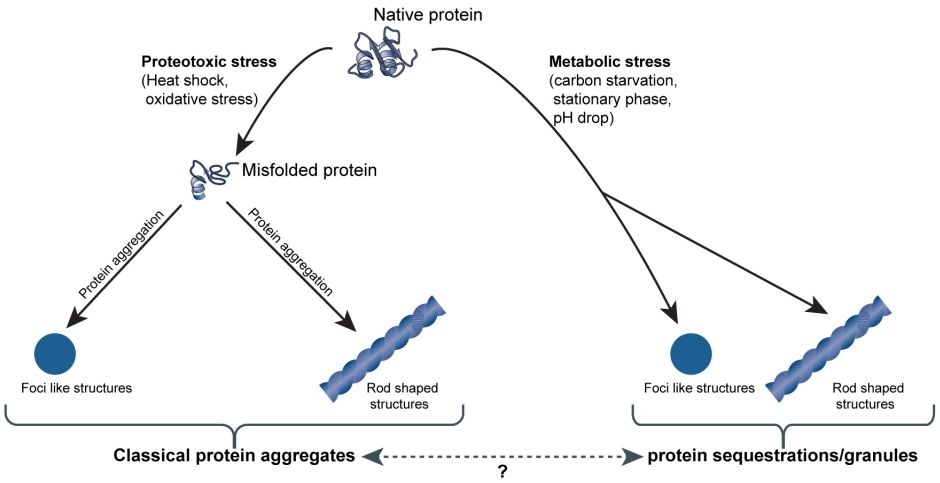

Figure 1.8: Relationship between classical protein aggregates and starvation induced granules is unclear.

Under proteotoxic stress, misfolded proteins accumulate resulting in the formation of protein aggregates, which appear either as foci (eg: VHL-mcherry) or rod shaped structures (eg: Sup35 prion) when viewed by light microscopy. Similarly, under starvation conditions that lead to changes in pH and availability of various metabolites amongst others, several proteins accumulate into foci or rod shaped structures in an unknown mechanism resembling microscopically those formed during proteotoxic stress. The relationship between these two kinds of protein sequestrations is however unclear, as indicated by the '?' mark in the cartoon above.

Notably, extending these observations, the ER exit marker Sec16 also reversibly accumulate into dense punctate structures in Drosophila cells upon depletion of serum

and amino acids [56]. Also, mitochondrial fragmentation in response to glucose depletion has been reported for mammalian cells [57]. Therefore, these observations extend the phenomenon of nutrient stress induced sequestrations from cytosolic proteins to organellar reporters.

Molecular chaperones such as Hsp104 and Hsp42 also accumulate into foci in stationary phase yeast cells, presumably suggesting increased protein misfolding and aggregation during quiescence [53]. Additionally, Hsp42 is required for the sequestration of Hos2 and Yca1 during starvation [58], similar to its role in driving aggregation during heat stress. A recent study implies that the majority of starvation-induced protein sequestrations represent aggregates of misfolded conformers [59].

In the light of such opposing suggestions made, the nature of these sequestrations and their relationship to classical protein aggregates remains unresolved (Figure 1.8).

1.4.1 Regulation of protein sequestrations by nutrient sensing pathways - Pre-autophagosomal structure (PAS) as a case study

Autophagy is a key cellular process that involves bulk engulfment of cellular components by double membrane structures leading to the formation of autophagosomes. Autophagosomes in turn fuse with the vacuole leading to the degradation of its contents. Formation of the double membrane structure termed as the phagophore, is thus central to the process and is achieved via mechanism analogous to the ubiquitin conjugating system whereby through a series of events a protein homologous to ubiquitin, termed Atg8, is conjugated covalently to phosphatidyl ethanolamine (PE) of the membrane. Such a process requires a concerted regulated localized activity of several autophagic proteins (Atgs), which is achieved by their accumulation that appears as one puncta in the cell that is termed as the Pre-autophagosomal structure (PAS). PAS is believed to be the site of autophagosome formation [47].

Atg1 is a key kinase regulating autophagy. Under non-starved conditions, TORC1 phosphorylates Atg13, which is an effector of Atg1 kinase, preventing its interaction with Atg1-Atg11-Atg20-Atg24 complex. As a consequence Atg1 kinase exhibits only basal activity. However, under starved conditions, TORC1 pathway gets inactivated and Atg13 is dephosphorylated aiding in its association with the Atg1-Atg11-Atg20-Atg24 complex. Interaction of Atg13 with the Atg1-Atg11-Atg20-Atg24 complex increases the kinase activity of Atg1, which is vital for orchestrating the assembly of other autophagic proteins (Atgs) at PAS (Figure 1.9) [47]. Additionally, direct phosphorylation of Atg1 via SNF1 kinase exerts a positive influence on Atg1 activity [Hedbacker2009]. Thus, TOR and SNF1 pathways converge together at Atg1 regulating sequestration of autophagic proteins at PAS and aiding in formation of autophagosomes. In agreement with the role of TOR pathway in autophagy, inhibition of TORC1 by a chemical, rapamycin, induces autophagy even in nutrient rich conditions [47]. Moreover, *tor1Δ* and *snf1Δ* cells are sensitive to nitrogen starvation, a condition traditionally used to induce autophagy [47, 60]further implying their role in autophagy.

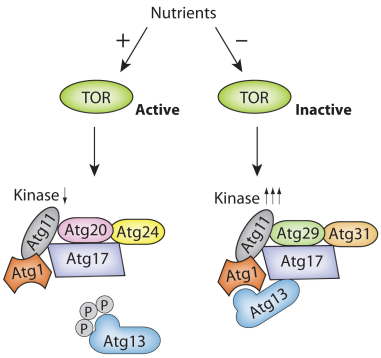

Figure 1.9: Regulation of Atg1 kinase activity by TOR kinase.
In the presence of nutrients, a condition that activates TOR kinase, Atg13 is phosphorylated reducing Atg13 affinity to the Atg1-Atg11-Atg20-Atg24 complex. Upon nutrient deprivation TOR becomes inactivated, leading to dephosphorylation of Atg13. This is followed by the assembly of Atg13 with Atg1 and with the Atg17-Atg29-Atg31 complex. The complex thus promotes an increase in Atg1 kinase activity and induction of autophagy. Adapted from [47].

1.4.2 Nutrient sensing pathways

There are numerous carbon and nitrogen sensing pathways found in yeast such as PKA, SNF1, Yak1, Sch9 and TOR [60]. While these pathways are known to cross-talk extensively, SNF1 and TOR pathways being the best understood, are discussed in greater details below.

1.4.2.1 SNF1 kinase pathway

SNF1 is Ser/Thr kinase. It is a multi subunit complex that is known to regulate cellular metabolism in response to changes in nutrient availability and environmental stress aiding in cellular adaptation and survival [60].

The core components of SNF1 kinase include snf1 and snf4 subunits. The core subunits can associate with any of the three cellular factors namely: 1) Sip1, 2) Sip2 and 3) Gal83, which determine the sub-cellular localization of the SNF1 kinase to vacuolar membrane, cytosol and nucleus respectively [60] (Figure 1.10). In the presence of glucose, SNF1 is localised to the cytosol while upon glucose depletion, it is targeted to different cellular localisations as determined by its above mentioned co-factors.

Regulation of SNF1 activity by glucose Under glucose limiting conditions, SNF1 is activated via phosphorylation of its snf1 catalytic subunit by upstream kinases such as Tos3, Elm1 and Sak1 [60]. The molecular mechanism of sensing glucose availability and its transduction to these above-mentioned kinases is poorly understood. Activated SNF1 auto-phosphorylates and phosphorylates several transcriptional factors (regulating expression of carboxylic acid cycle and β-oxidation of fatty acids), metabolic enzymes (such as Acc1, inhibiting its activity) and thereby regulate their activity contributing to metabolic reprogramming and aiding in cellular adaption to availability of glucose among other nutrients. Upon addition of glucose, SNF1 is dephosphorylated via Glc7-Reg1 phosphatase rendering it inactive (Figure 1.10)[60]. In a mechanism that is poorly understood, the Hsp70 Ssb is known to aid in inactivating SNF1 [44]. Thus glucose availability is coupled efficiently to SNF1 activity status.

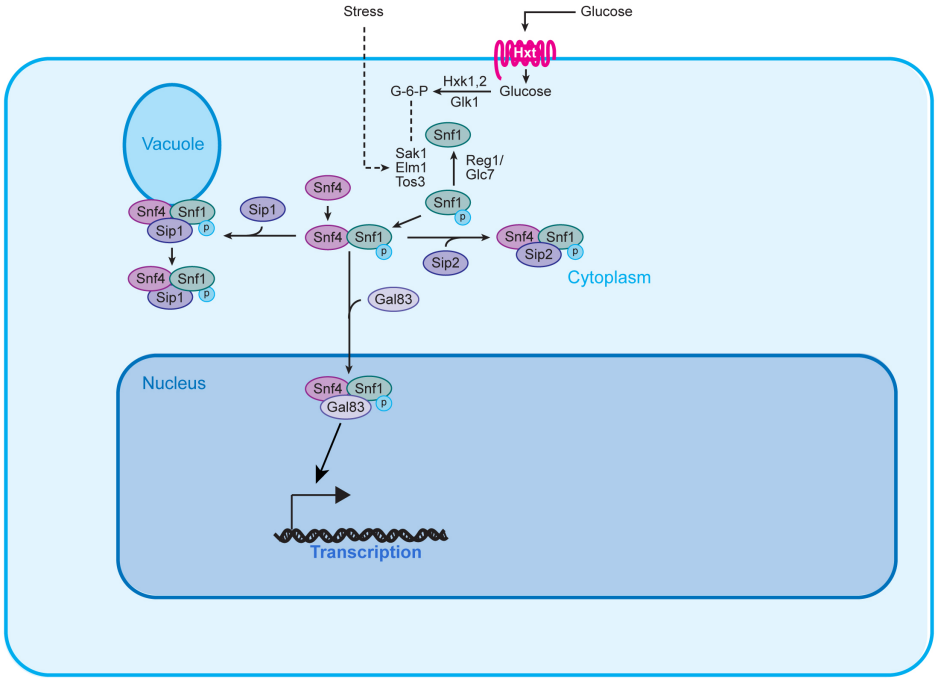

Figure 1.10: SNF1 mediated glucose sensing.

SNF1 kinase depending on the associated co-factors (Sip1, Sip2 and Gal83) is localised to either vacuole, cytosol and nucleus respectively. The role of SNF1 at the vacuole is unknown. In the nucleus, it is known to regulate the expression of numerous genes involved in carboxylic acid cycle and β-oxidation of fatty acids in response to glucose availability. SNF1 also modulates the activity of several metabolic enzymes in the cytosol and thereby modulates adaptation of cells to changing glucose availability. Adapted from [60].

1.4.2.2 TOR signaling pathway

TOR (Target of Rapamycin) signaling being one of the key nutrient sensing pathways co-ordinates nutrient availability with the metabolic status of cells whilst cross-talking extensively with other nutrient sensing pathways. There are two functional complexes that together constitute the TOR pathway components. They are: TORC1 and TORC2 complexes. Each of these two functional complexes exists as dimers. TORC1 complex monomer comprises either Tor1 or Tor2 together with Lst8 and Kog1 while TORC2 complex monomer comprises of Tor2, Lst8, Avo1, Avo2 and Avo3 [61, 60](Figure 1.11).

The two TOR complexes apart from differing in their subunit composition, also differ in their functions (Figure 1.11). While TORC1 complex regulates translation initiation via phosphorylation of eIF4E, transcription and autophagy, the TORC2 complex regulates actin reorganization and sphingolipid biosynthesis [61, 60]. Given the pace at which TOR signaling is becoming implicated in regulating new cellular activities, it is clear that its functions are not exhausted.

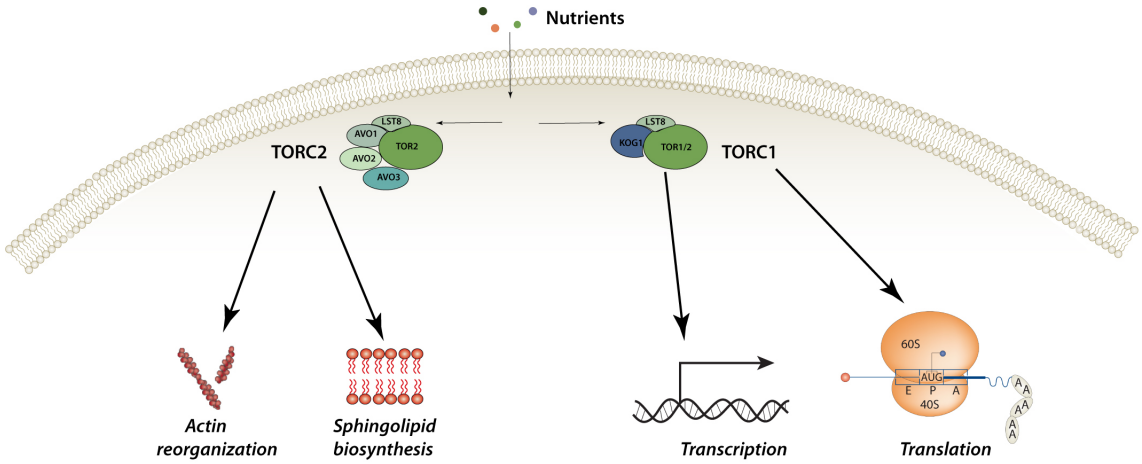

Figure 1.11: Functions of TOR pathway.

TOR signalling consists of two functional complexes, namely, TORC1 and TORC2. While TORC1 complex regulates translation initiation, transcription and autophagy, the TORC2 complex regulates actin reorganization and sphingolipid biosynthesis.

1.5 Aims of this work

Sequestration of proteins is a conserved principle in living systems. On the one hand, it aids in facilitating temporal and localized control of protein activity. On the other hand, it can isolate potentially unwanted or toxic proteins from their healthy counterparts. Metastable proteins and nascent polypeptides can misfold under conditions of proteotoxic stress resulting in the formation of toxic protein aggregates. It is becoming increasingly clear that a dedicated set of quality control factors aid in formation and deposition of protein aggregates and represents a classical demonstration of the latter role of protein sequestrations.

In recent years, it is becoming evident that several metabolic enzymes and stress factors sequester reversibly under conditions of metabolic stress, such as nutrient limitation. Very little is known regarding the nature of these sequestrations and their physiological relevance. Several reports present contrasting views of these sequestrations. Accordingly, these sequestrations are believed to represent: 1) inactive storage assemblies; 2) protein assemblies for localized activity or 3) protein aggregates.

Given the controversial view on metabolic stress induced sequestrations, it is vital to perform a systematic study of the nature of these sequestrations in relationship to classical protein aggregates. In S.cerevisae, Fatty acid synthetase (FAS) subunits being prone to sequestration under conditions of both known proteotoxic and metabolic stress (nutrient limitation) provide an ideal model system for such a study. The key questions that are raised using this model system are: 1) characterization of metabolic stress induced FAS sequestration and its relationship to misfolded protein aggregates; 2) their relative cellular localization; 3) generality of the phenomenon of co-sequestration of functionally related proteins and 4) physiological significance of starvation induced sequestrations.

2 Results

2.1 Fas1 and Fas2 co-sequester upon prolonged starvation into distinct foci

Fas2p, one of the two subunits of FAS was reported to sequester into foci in stationary phase cells [53]. The fate of the other subunit, Fas1p and thus the intact FAS complex under starvation conditions is unknown. In order to follow the fate of the entire complex, both the subunits of FAS (Fas1 and Fas2) were genomically tagged with different fluorescent markers (GFP or mcherry) and their localization monitored by fluorescence microscopy. During logarithmic growth, both subunits exhibited a diffuse cytosolic distribution while co-accumulating into mainly one focus when the cells entered quiescence stage upon prolonged growth in stationary phase (Figure 2.1A). Co-localization studies with other reported markers (Gln1-mcherry, Ura7-GFP, Pre6-GFP and Ade4-GFP) known to form foci or rods during quiescence[53][51, 52] revealed that Fas1-mcherry/Fas1-GFP is sequestered at a site distinct from these sequestrations (Figure 2.1C). Additionally, Fas1-mcherry is sequestered much later (similar to Gln1-mcherry) unlike Ura7-GFP, Pre6-GFP or Ade4-GFP that are sequestered very early during stationary phase (Figure 2.1D). When an alternate form of metabolic stress such as glucose depletion was used, Fas1-mcherry also accumulated into foci. Here, multiple Fas1-mcherry foci formed at a faster rate as compared to stationary phase (Figure 2.2A-B). We confirmed Fas1 foci formation upon glucose depletion by immunofluorescence against a C-terminally myc-tagged Fas1 to exclude the possibility of FAS sequestration to be artificially caused by tagging to fluorescent probes (Figure 2.2C).

To gain insight into the nature of the distinct FAS sequestration and its sub-cellular localization, correlative electron microscopic analysis of glucose depletion induced Fas1-mcherry foci was performed. Fas1-mcherry foci represent ribosome free zones in the cytosol indicating tight packing of individual Fas1-mcherry molecules in the foci (Figure 2.2D). I did not observe any obvious association of Fas1-cherry foci with organelles or membrane structures. Similar results were obtained when Fas1-mcherry localization was determined by immuno electronmicroscopy (Figure 2.2E). In log-phase cells gold particles, labeling FAS, were evenly distributed throughout the cytosol, whereas in starved cells gold particles formed discrete clusters, which do not show apparent specific association with cellular structures.

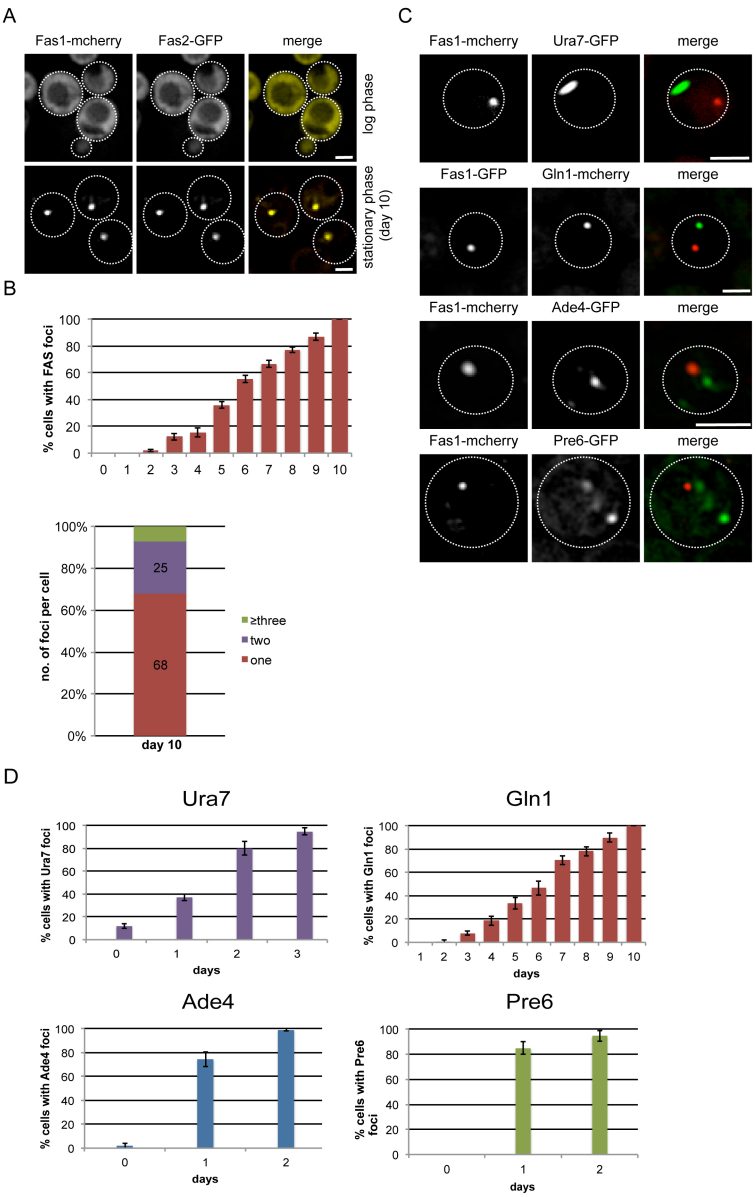

Figure 2.1: Fas1 and Fas2 co-sequester into distinct foci upon prolonged starvation.

(A) Both subunits of FAS co-sequester into foci that co-localize in stationary phase cells. *S.cerevisiae* cells expressing Fas1-mcherry and Fas2-GFP were grown to log phase or stationary phase (10 days) at 30°C. Changes in protein localizations were recorded. Dashed lines indicate cell boundaries. Single Z-plane images are shown. Bars, 2 µm. (B) Time dependent changes in the percentage number of cells harboring FAS foci in cells grown to late stationary phase at 30°C. FAS accumulates into mainly one focus in the cell.Percentage distribution of number of Fas1-mcherry foci per cell in stationary phase cells grown for 10 days in SD medium at 30°C. (C) FAS is sequestered at a site distinct from other known sequestrations. *S.cerevisiae* cells co-expressing Fas1-mcherry/Fas1-GFP with Ura7-GFP, Gln1-mcherry, Ade4-GFP or Pre6-GFP were grown to stationary phase in SD medium for 10 days at 30°C. Localizations of proteins were determined by fluorescence microscopy. Single Z-plane images are shown. Bars: 2 µm. (D) Proteins sequester at different rates in stationary phase. Cells expressing Ura7-GFP/Gln1-mcherry/Ade4-GFP /Pre6-GFP were grown to stationary phase in SD medium. Time dependent changes in the percentage number of cells harboring foci for the above mentioned proteins were determined. The experiments were repeated twice and standard deviations are given.

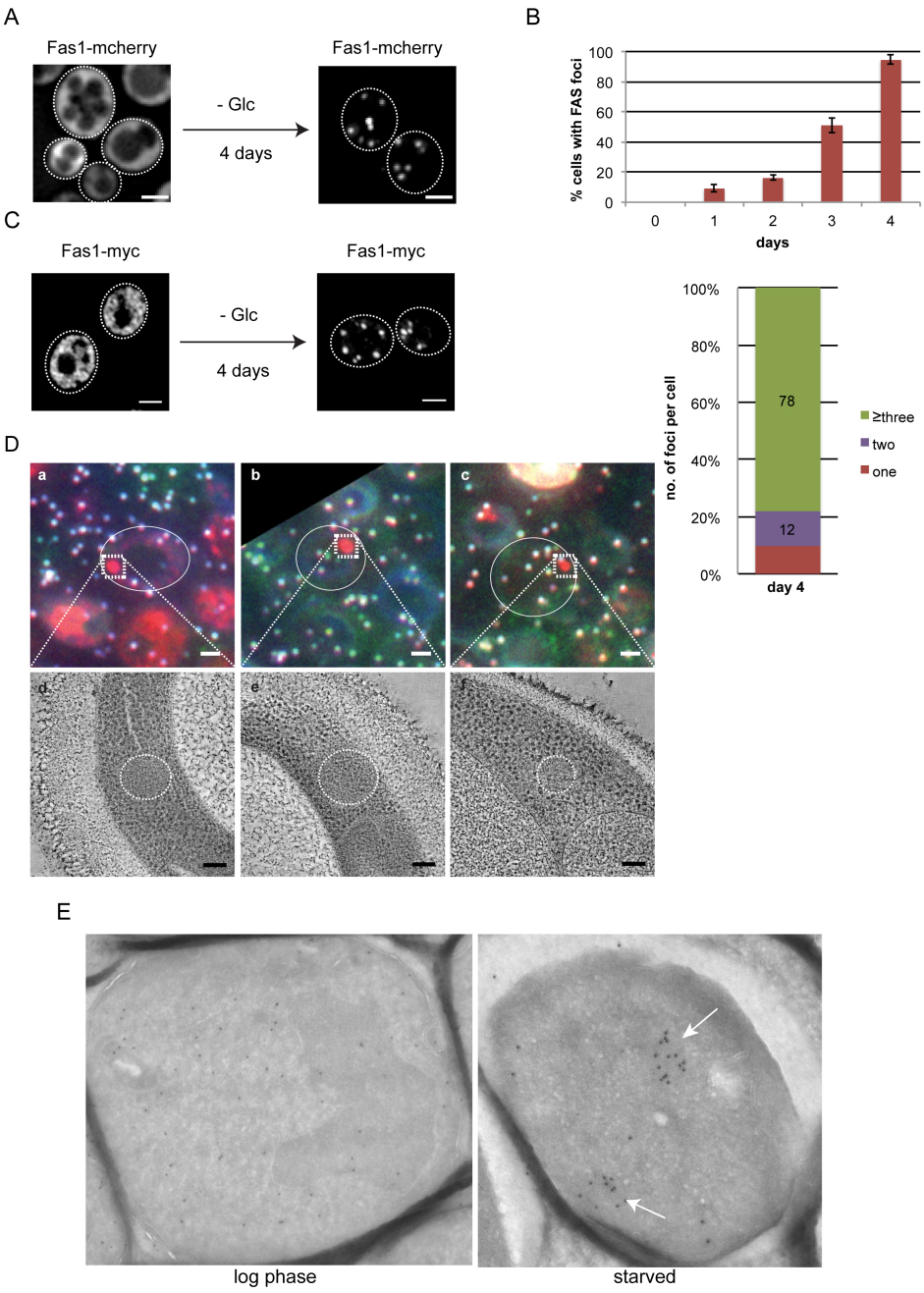

Figure 2.2: FAS is sequestered into multiple foci upon glucose starvation.

(A) Fas1-mcherry accumulates into multiple foci upon prolonged glucose depletion. (B) Kinetics of Fas1-mcherry foci formation in cells starved of glucose for 4 days. (C) Fas1 accumulates into foci upon glucose depletion. Fas1-7xmyc tagged cells were either grown to log phase or glucose starved for 4 d and localisation of Fas1 was probed by immuno-fluorescence using anti-myc antibody. (D) Fluorescence correlated electron microscopic analysis of Fas1-mcherry foci formed upon glucose depletion. (a-c) An overlay of GFP, mcherry and blue fluorescence channels to visualize Fas1-mcherry spots as well as fiducial, which are visible in all three channels in three different cells. Circles mark the boundary of the cell and the foci are marked by dashed squares. (d-e) are close-up views of virtual slices through the tomogram, corresponding approximately to the boxed areas in (a-c), respectively. (E) Immuno-EM analysis of FAS foci using an anti-FAS antibody. Dark spots represent immuno-gold particles. Scale bars: 500 nm. Scale bars: 2 µm in A-C. 1 µm in D (a-c) or 100 nm in D (d-f). 500 nm in E.

2.2 FAS sequestrations are dynamic and do not represent protein aggregates

I next analyzed the relationship of starvation-induced FAS sequestrations to protein aggregates. Hsp104, the AAA+ protein disaggregase in yeast is known to refold aggregated proteins in co-operation with the Hsp70 system and is thus a reliable marker for protein aggregates. Fluorescence microscopic analysis revealed functional Hsp104-GFP to form multiple foci in stationary phase cells that do not co-localize with Fas1-mcherry foci indicating that Fas1 sequestration are not classical protein aggregates (Figure 2.3A). Fas1-mcherry also formed foci in quiescent *hsp42Δ* cells, supporting a non-aggregate like nature of FAS sequestration (Figure 2.3B). We also considered the possibility that FAS foci are not substrate of the Hsp104 disaggregase but are cleared from cells by autophagy. Co-expression of Fas1-GFP and Ape1-mcherry, a marker for the pre-autophagosomal structure (PAS), did not reveal co-localization of both proteins upon starvation (Figure 2.3C). Together these findings suggest that FAS foci do not represent accumulation of misfolded proteins subjected to protein quality control.

To further characterize FAS foci I determined their dynamics by Fluorescence loss in photobleaching (FLIP) experiments. Here, a small area of the stationary phase cells far away from the Fas1-mcherry foci was continuously bleached and the fluorescence intensity of the foci was monitored in parallel. Fluorescence intensity of the Fas1-mcherry foci dropped rapidly over the period of bleaching indicating a rapid exchange of Fas1-mcherry molecules between the foci and the cytosol, separating FAS foci from immobile cytosolic protein aggregates (Figure 2.3D).

Resolubilisation of some of the stationary phase induced sequestrations upon addition of specific nutrients has been reported[53][51]. I therefore analyzed the fate of FAS foci upon addition of nutrients. Addition of fresh complete medium (SD medium) induced Fas1-mcherry foci to rapidly dissolve and to re-distribute itself uniformly in the cytosol (Figure 2.3E). Foci disintegration was completed after 120 min in most cells. The simultaneous addition of cycloheximide did not prevent FAS foci disintegration demonstrating that the solubilization does not rely on protein synthesis and that the regained diffuse Fas1-mcherry fluorescence originates from the starvation induced sequestrations. In order to determine the minimal requirement for the resolubilisation of Fas1-mcherry foci, a series of addition experiments were performed wherein either one or a combination of media components were added to the starved cells. Glucose alone was sufficient to trigger the resolubilisation of Fas1-mcherry foci while other media components individually or in combination did not (Figure 2.3E). Non-metabolisable glucose analogue, 2,4-deoxyglucose did not allow this resolubilisation indicating that metabolizing glucose is a prerequisite for the disintegration of Fas1-mcherry foci (data not shown). Resolubilisation of Fas1-mcherry foci upon glucose addition was not perturbed in *hsp104Δ* cells, confirming that FAS foci are not protein aggregates (Figure 2.3F).

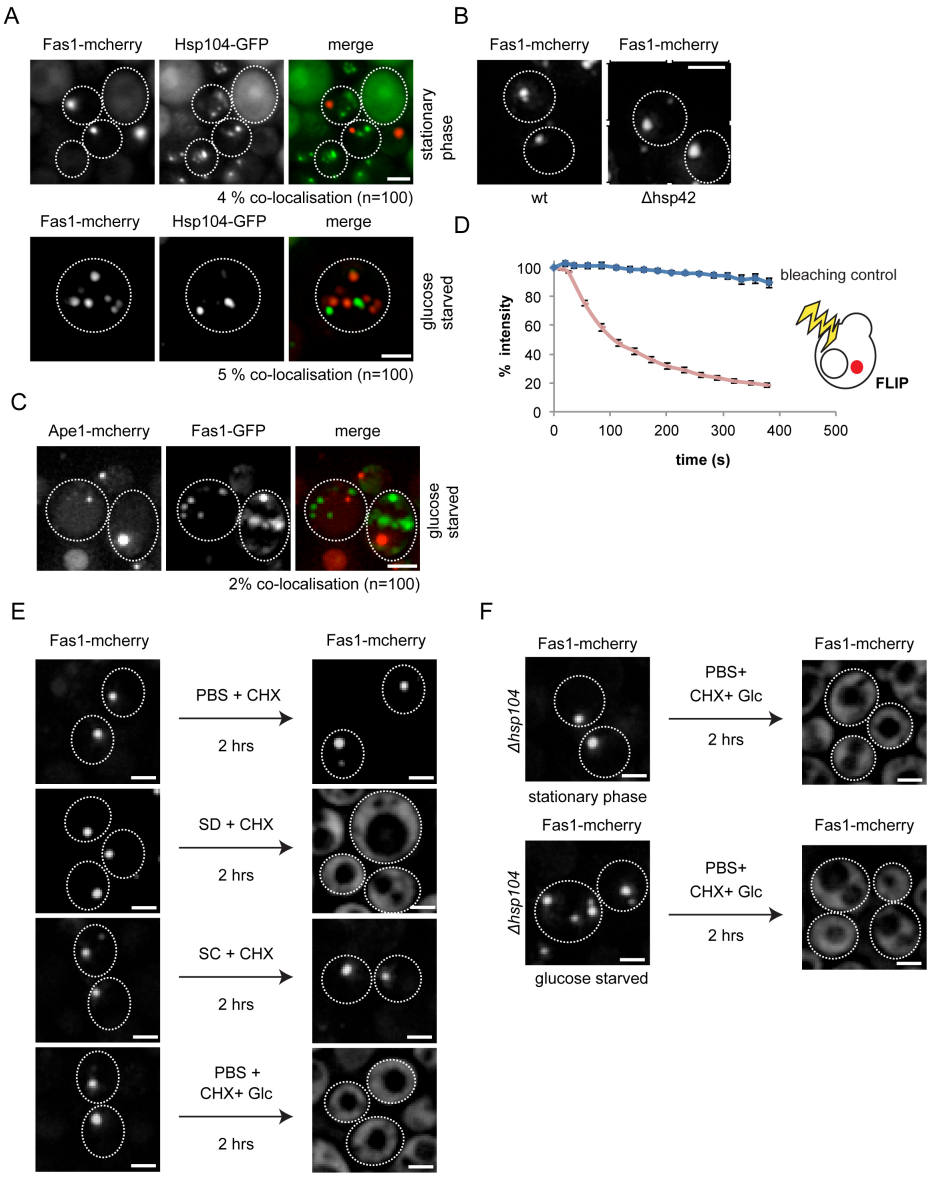

Figure 2.3: FAS sequestrations are dynamic and not classical protein aggregates.

(A)S. cerevisiae cells expressing Fas1-mcherry and Hsp104-GFP were grown to stationary phase (day 10) or depleted for glucose (day 4). Single Z-plane images (upper panel) or maximum intensity projections of Z-stack images (lower panel) are shown. Bars: 2 µm. (B) S. cerevisiae wt or *hsp42Δ* cells continue to sequester Fas1-mcherry when grown to stationary phase.Bars: 2 µm. (C) S. cerevisiae cells expressing Fas1-GFP and Ape1-mcherry were grown to stationary phase (day 10). Bars: 2 µm. (D). FLIP measurements of Fas1-mcherry foci formed in stationary phase cells. Standard deviations are given (n=20). (E) Fas1-mcherry sequestration is reversible. S. cerevisiae cells harboring Fas1-mcherry foci after growth to stationary phase were resuspended in either PBS buffer, fresh SD medium, fresh SC medium or PBS buffer containing 2% (w/v) glucose. Cycloheximide (CHX) was added to block new protein synthesis. Bars: 2 µm. (F) S. cerevisiae *hsp104Δ* cells expressing Fas1-mcherry were either grown to stationary phase (day 10) or glucose depleted (day 4) to induce Fas1-mcherry foci and were resuspended in PBS buffer containing 2% (w/v) glucose to induce resolubilisation of the foci. Bars: 2 µm.

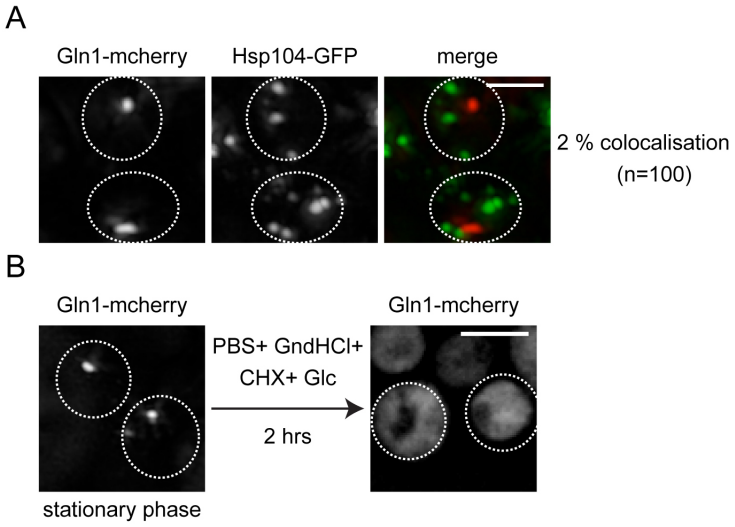

Figure 2.4: Gln1 foci formed during stationary phase are not protein aggregates.

(A) *S. cerevisiae* wt cells expressing Gln1-mcherry and Hsp104-GFP were grown to stationary phase for 10 days at 30°C. The degree of co-localization was determined. (B) *S. cerevisiae* cells harboring Gln1-mcherry foci after growth to stationary phase were resuspended in either PBS buffer containing 2% (w/v) glucose. Cycloheximide (CHX) was added to block new protein synthesis and addition of Guanidinium hydrochloride (GdnHCl) inhibits Hsp104 activity. Changes in protein localizations were determined. Maximum intensity projections of Z-stack images are shown. Bars: 2 µm.

My presented findings differ from a recent study, suggesting the majority of starvation induced protein inclusions including Gln1 to be aggregates of misfolded protein conformers[59]. In view of this discrepancy I re-analyzed starvation induced foci formation and disintegration of Gln1-mcherry (Fig. 1.4). Gln1-mcherry forms foci in starved yeast cells, which do not co-localize with Hsp104-GFP (Figure 2.4A). Readdition of glucose led to rapid resolubilization of preexisting Gln1 foci. The simultaneous addition of cycloheximide and guanidinium hydochloride (GdHCl), a potent inhibitor of Hsp104 activity, did not abrogate Gln1-mcherry foci disintegration (Figure 2.4B). Together these findings provide strong evidence that starvation induced Gln1 inclusions also do not represent protein aggregates.

2.3 Metabolic status of cells regulate the sequestration of FAS

Given that FAS foci do not represent protein aggregates and are formed upon prolonged nutrient limitation, I speculated that the metabolic status of cells regulates the kinetics of FAS sequestration. Nutrient sensing pathways including TOR and Snf1 pathways govern the metabolic status of cells by regulating several key metabolic enzymes in response to changes in nutrient availability [60]. Mitochondria, being a key source of ATP production and a major contributor for various metabolic pathways, is another key regulator of cellular metabolic status. I therefore tested FAS sequestration in mutants of TOR and Snf1 signalling pathway (*tor1Δ* and *reg1Δ*) as well as in rho minus cells lacking mitochondria. In all the mutant strains, we observed a substantially faster sequestration of FAS (Figure 2.5A). FAS foci were still reversed by the addition of glucose, demonstrating that only the kinetics of formation but not the nature of FAS foci is changed in the mutant cells (Figure 2.5B). Together, the data hints the metabolic status of cells to be a key contributor regulating the sequestration of FAS upon nutrient limitation.

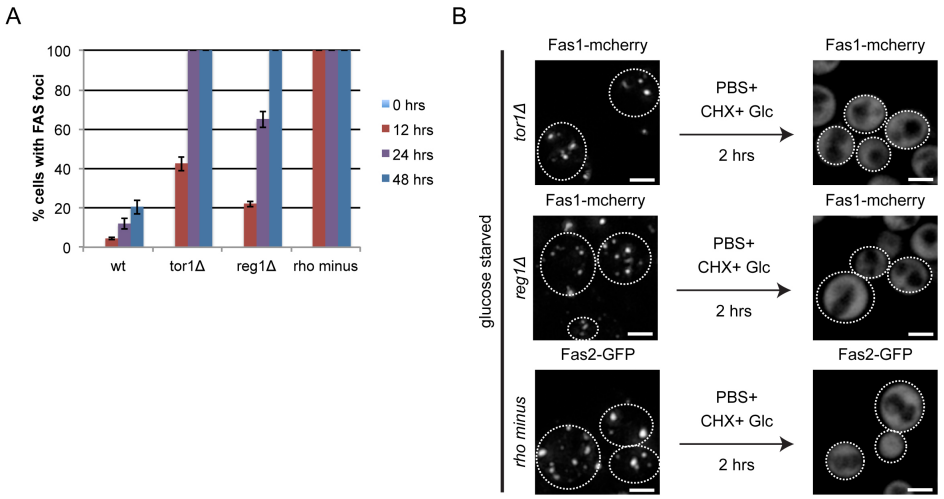

Figure 2.5: Nutrient sensing pathways affect the kinetics of FAS sequestration.

(A) wt, *tor1Δ*, *reg1Δ* and rho minus cells expressing Fas1-mcherry/Fas2-GFP were grown to log phase and subsequently starved of glucose by transferring them to media lacking glucose. Changes in localization of FAS monitored by fluorescence microscopy at different time points and their kinetics determined. Standard deviations are given (n=2). (B) FAS foci formed in nutrient sensing mutants are reversible. Glucose starved *tor1Δ*, *reg1Δ* and rho minus cells expressing Fas1-mcherry/Fas2-GFP were replenished with glucose in the presence of cycloheximide (100 µg/ml) and changes in localization monitored by fluorescence microscopy. Images represent maximum intensity projection of the Z-stack images. Bars: 2 µm.

2.4 Co-translationally acting chaperones, Ssb and NAC affect FAS sequestration

Ssb, a ribosome associated Hsp70 chaperone aiding in co-translational protein folding, was recently implicated in regulating SNF1 activity status [44]. Ssb was shown to render SNF1 inactive in a mechanism that is not understood[44]. Given that I observed faster kinetics of FAS sequestration in *reg1Δ* cells, I wanted to test whether *ssbΔ* (*ssb1Δ ssb2Δ*) cells also sequester FAS at a faster rate. Indeed, I observed that FAS is sequestered into multiple foci with a much faster kinetics in *ssbΔ* stationary phase cells, that are resolubilised upon addition of glucose (Fig.1.6A-B). Moreover, unlike in wild type and *reg1Δ* cells, Fas1-mcherry sequestered into multiple foci in *ssbΔ* cells. In order to test whether the observed effect in ssbΔ cells on FAS sequestration was through ssb's proposed role in regulating SNF1 kinase activity, FAS sequestration was monitored in *ssbΔsnf1Δ* cells. Fas1-mcherry continued to sequester into reversible multiple foci in *ssbΔsnf1Δ* indicating that the observed effect on FAS sequestration in *ssbΔ* cells cells was SNF1 independent. It is therefore possible that the chaperone action of Ssb is necessary for FAS sequestration.

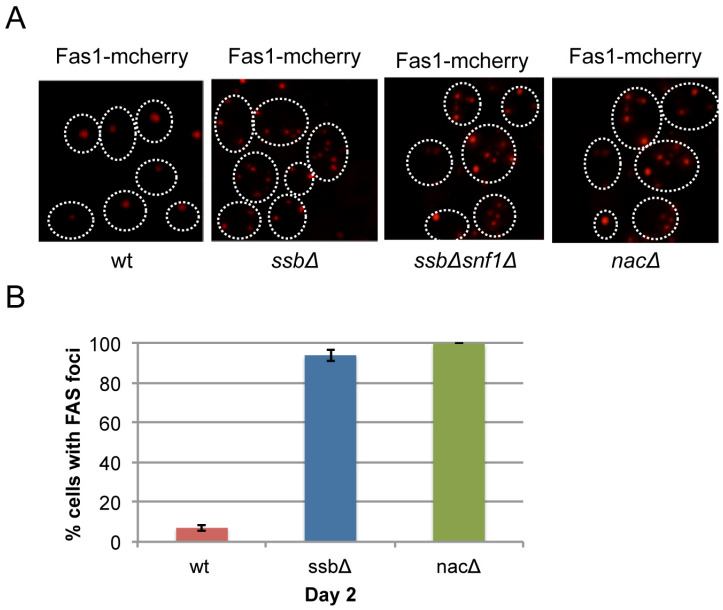

Figure 2.6: Ssb and NAC affect FAS sequestration.

(A) wt, *ssbΔ, ssbΔsnf1Δ and nacΔ* cells expressing Fas1-mcherry were grown to stationary phase in SD medium at 30°C. Changes in localisation of Fas1-mcherry was monitored by fluorescence microscopy. Fas1-mcherry accumulates into multiple foci in *ssbΔ, ssbΔsnf1Δ* and *nacΔ* cells unlike wt cells which accumulate Fas1-mcherry into mainly one focus. (B) Kinetics of foci formation was determined. Standard deviations are given (n=2). Scale bar: 2 µm.

NAC (Nascent chain associated complex) like Ssb, is another ribosome associated chaperone known to aid in co-translation protein folding and targeting. Given that

2.4 Co-translationally acting chaperones, Ssb and NAC affect FAS sequestration

Ssb affects FAS sequestration, I tested for possible effects on Fas1-mcherry sequestration in *nacΔ* (*egd1Δ egd2Δ btt1Δ*) cells. Indeed, like ssbΔ cells, Fas1-mcherry reversibly sequesters into multiple foci at faster kinetics in *nacΔ* stationary phase cells (Fig.). Therefore, co-translationally acting chaperones (Ssb and NAC) tend to affect the kinetics and number of FAS sequestration in stationary phase cells. Further work needs to be done to explore their functions in regulating global protein sequestrations and molecular mechanisms that govern them.

2.5 Mutants affecting the integrity of the secretory pathway affect FAS sequestration

While FAS sequestrations seems to be affected by the metabolic status of cells, I wondered if FAS sequestration could also be triggered by other forms of stress such as membrane stress. I therefore analyzed a number of well characterised mutants (*sec17-1,sec22-3, sec9-4, ubp3Δ*) that are defective in different steps of the secretory pathway[62]. Indeed, in all the tested secretory pathway mutants, I observed a faster rate of FAS sequestration upon entry into stationary phase with *sec17-1* mutant exhibiting the strongest effect (Figure 2.7A). It must be noted that this effect was observed already under permissive temperatures and got slightly more pronounced under restrictive temperature. FAS sequestration remained reversible upon addition of glucose in all these mutants tested.

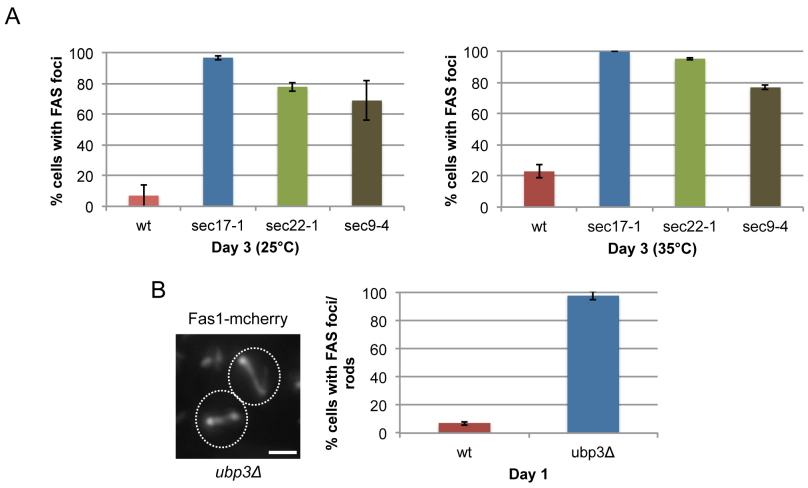

Figure 2.7: Secretary pathway mutants affect kinetics of FAS sequestration.

(A) wt, *sec17-1, sec22-3,Sec9-4* cells expressing Fas1-mcherry were grown to stationary phase in SD medium at either 25°C (permissive temperature) or 35°C (non-permissive temperature). Changes in localisation of Fas1-mcherry was monitored by fluorescence microscopy. Kinetics of foci formation were determined for different strains. Standard deviations are given (n=2). (B) Wt and *ubp3Δ* cells were grown to stationary phase in SD medium at 30°C. Changes in localisation of Fas1-mcherry was monitored. Fas1-mcherry accumulates into rods in *ubp3Δ* cells. Kinetics of rod formation was determined.Standard deviations are given (n=2). Scale bar: 2 µm.

While FAS is sequestered at a much faster rate in *ubp3Δ* cells when grown to stationary phase like other secretory pathway mutants, FAS is sequestered into rod shaped structures in *ubp3Δ* cells (Figure 2.7B), which are reversible upon addition of glucose.

2.6 FAS sequestration is not essential for cellular survival upon prolonged glucose starvation

Given that FAS sequestrations formed upon nutrient limitation are not protein aggregates, I analyzed whether FAS foci reflect an adaptive response of cells that would aid them to survive starving conditions. I therefore aimed at monitoring the viability of cells in which FAS is no longer sequestered into cytosolic foci under glucose starvation. To achieve this, I exploited the 'anchor-away technique'[63], wherein any freely diffusing protein could be targeted to a particular cellular compartment in an inducible fashion upon addition of the drug rapamycin. Here, Fas1 was genetically tagged to FRB-GFP protein at the C-terminus in a rapamycin resistant strain where the plasma membrane protein Pma1 was genetically tagged to FKBP12 at its C-terminus. I genetically tagged Fas2 with mcherry at its C-terminus to follow the localization of the entire FAS complex. Both the subunits, Fas1-FRB-GFP and Fas2-mcherry, which showed cytoplasmic localization in logarithmic growth, are anchored away within minutes to the plasma membrane upon addition of rapamycin (Figure 2.8A). Thus, by pulling on Fas1, the intact FAS complex is targeted to the plasma membrane. Therefore, I subsequently monitored Fas2-mcherry as a read-out for localization of the intact FAS complex.

Cells were grown to logarithmic growth phase and subsequently starved of glucose with or without addition of rapamycin. In the chosen strain background cytosolic FAS foci formed already after one day of glucose depletion. These foci were present in the cytosol of untreated control cells, while Fas2-mcherry remained anchored away at the plasma membrane in rapamycin treated cells (Figure 2.8B). Notably, under starvation conditions the membrane staining by Fas2-mcherry became less smooth and some membrane-bound foci were apparent. I subsequently tested the viability of cells at different time points by spotting assays (Figure 2.8C) and a more sensitive, dead cell staining dye (sytox green) based Fluorescence-activated Cell sorting (FACS) of cells (Figure 2.8D). Strains wherein Fas1 is not tagged to FRB and thus cannot be anchored to the plasma membrane were used as control for any indirect effect of rapamycin on cell viability. By both methods, I do not observe any significant effect on cell viability upon prevention of FAS sequestration. I conclude that the formation of cytosolic FAS foci is not essential for cellular survival upon prolonged glucose starvation.

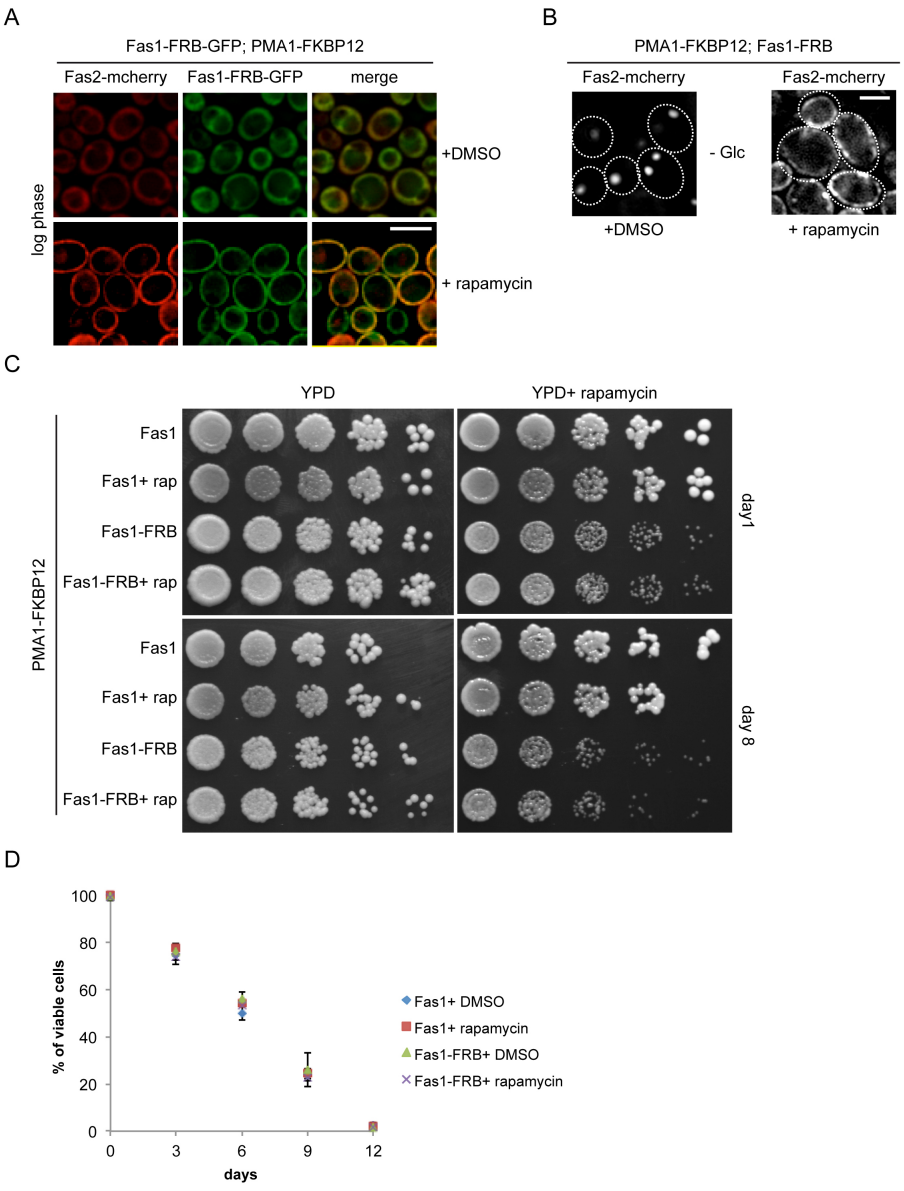

Figure 2.8: FAS sequestration is not essential for cellular survival upon prolonged glucose depletion.

(A/B) Rapamycin resistant *S. cerevisiae* cells expressing PMA1-FKBP12, Fas1-FRB-GFP and Fas2-mcherry were grown at 30°C to log phase in SD medium (A) or were depleted from glucose (B). Cells were either treated with DMSO or rapamycin. In rapamycin treated cells, both Fas1-FRB-GFP and Fas2-mcherry are targeted to PMA1-FKBP12 at the plasma membrane, while both subunits retain cytoplasmic localization in DMSO treated control cells (A). Upon glucose starvation control cells (+ DMSO) form cytosolic Fas2-mcherry foci, while rapamycin addition keeps Fas2-mcherry at the membrane (B). (C/D) In rapamycin resistant S. cerevisiae cells co-expressing PMA1-FKBP12 and Fas2-mcherry, Fas1 was either genomically tagged FKBP12 or not. Both strains were grown to log phase at 30°C in SD medium and depleted from glucose by transferring them to SC medium. DMSO (control) or rapamycin was added upon glucose depletion. Cell viability was measured for all cells by spot tests on YPD and YPD + rapamycin plates (C) and by sytox green staining based FACS sorting of dead cells (D).

2.7 FAS foci are enzymatically active and do not colocalize with enzymes involved in fatty acid or lipid biosynthesis

The physiological meaning for sequestering FAS during quiescence is unknown. I could envision the following two scenarios: i) FAS sequestration might represent an inactive enzyme storage assembly formed under nutrient limiting conditions or ii) a strategy for active recruitment of enzymes to facilitate localized synthesis of fatty acids and phospholipids.

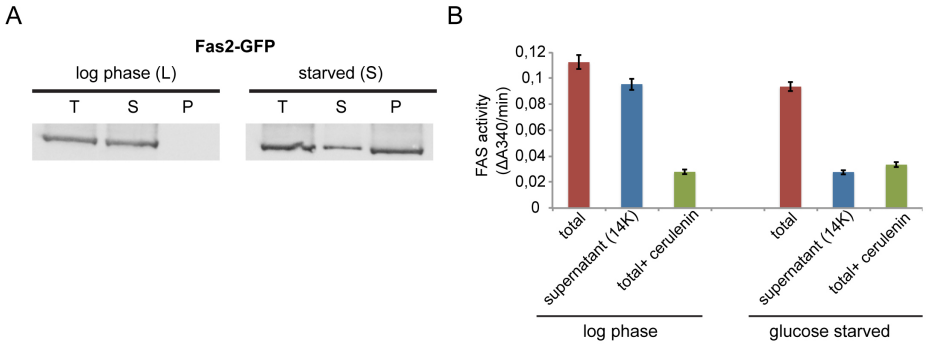

Figure 2.9: FAS foci are enzymatically active.

(A) *S. cerevisiae* cells expressing Fas2-GFP were grown at 30°C to either log phase or were depleted of glucose for 4 days to induce Fas2-GFP foci. Total cells lysates (T) were separated into soluble (S) and insoluble (P) fractions by centrifugation. Distribution of Fas2-GFP was determined by western blot analysis using GFP-specific antibodies. (B) FAS activity was determined in total and soluble cell fractions of log phase and glucose starved cells. Activity determined in presence of FAS inhibitor Cerulenin indicates background conversion of NADPH by other cellular components. Standard deviations are given (n=2).

In an attempt to distinguish between the two possibilities, I monitored the activity of FAS in crude cell lysates. The activity assay was based on the observation that the majority of Fas2-GFP foci could be efficiently pelleted by centrifugation in starved cells while it remained in the soluble fraction in the log phase cultures (Figure 2.9A). Thus by comparing FAS activity of total cell extracts with that of soluble fractions upon centrifugation, we could decipher the activity status of Fas2-GFP in foci. In log phase cells most of the activity of the Fas2-GFP determined in the total extracts was retained in the soluble fraction correlating with the presence of diffuse Fas2-GFP fluorescence (Figure 2.9B). In starved cells, FAS activity was determined in total cell extracts and was comparable to those observed in log phase cells. However, FAS activity was largely lost upon centrifugation and dropped to background activity levels that were still determined in presence of the FAS inhibitor Cerulenin (Figure 2.9B). Together these findings demonstrate that FAS sequestrations formed during starvation retain enzymatic activity. This observation potentially supports a model in which FAS sequestration represents an act of active recruitment for localized synthesis rather than for storage. I therefore analyzed whether other enzymes

involved in fatty acid and phospholipid biosynthesis also experience spatial reorganization during starvation, potentially leading to clustering in close vicinity to FAS foci (Figure 2.10A). I monitored cytosolic Acc1, which synthesizes Malonyl-CoA that is used as substrate by FAS. I also followed the localizations of ER-resident Pis1, mitochondria-resident Psd1 and Erg6, present in lipid droplets. These enzymes use fatty acids, the products of FAS activity, for phospholipid and ergosterol biosynthesis. Genomic C-terminal fusions of the above enzymes were created to either GFP or mcherry fluorescent monitors and analyzed by fluorescence microscopy. Functionality and correct localization of all fusions was ensured (Acc1, Pis1) or reported by others (Erg6, Psd1) [64][65]. While all the enzymes showed their typical subcellular localization in log phase cultures, they accumulated into punctate or rod-like (Acc1) structures during glucose starvation (Figure 2.10A). Pis1-3xmcherry (ER), Psd1-3xmcherry (mitochondria) and Erg6-GFP (lipid droplets) precede in accumulating into punctate structures and are followed by the sequestration of cytosolic Acc1-GFP and Fas1-mcherry (Figure 2.10B). Thus sequestration of enzymes involved in phospholipid and fatty acid biosynthesis are different with the latter sequestering more slowly. Importantly, all tested enzymes, while being sequestered upon starvation, never co-localized, indicating that clustering of functionally related enzymes during starvation is not a conserved phenomenon. Together these data rather support FAS foci representing storage assemblies of native subunits, which retain enzymatic activity that is, however, not increased compared to free FAS and is not linked to enzymes acting upstream or downstream of FAS.

2.7 FAS foci are enzymatically active and do not colocalize with enzymes involved in fatty acid or lipid biosynthesis

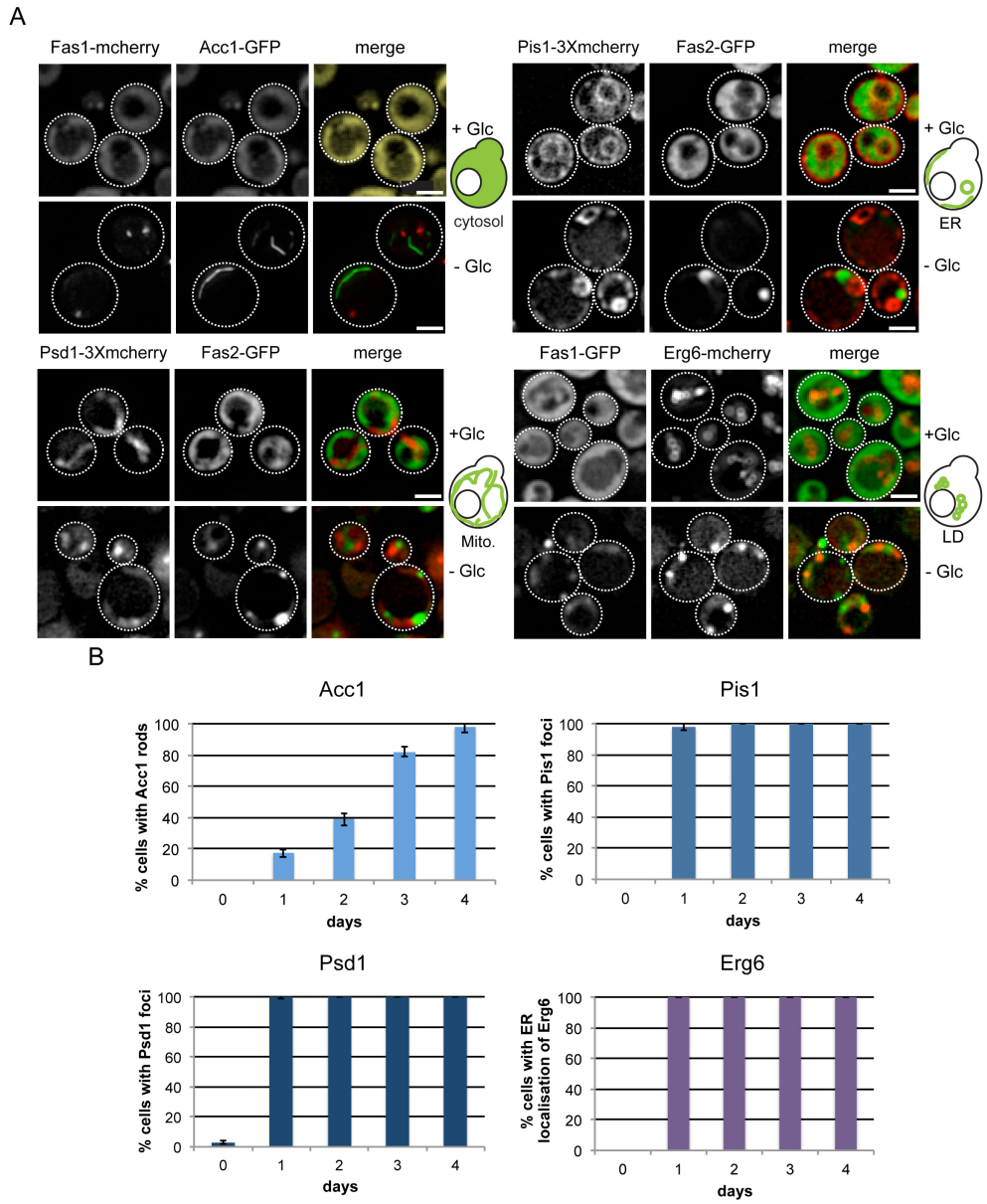

Figure 2.10: Lipid biosynthetic enzymes do not co-cluster upon glucose starvation.

(A) *S. cerevisiae* cells co-expressing either Fas1-mcherry and Acc1-GFP, Fas2-GFP and Pis1-3Xmcherry, Fas2-GFP and Psd1-3Xmcherry or Fas1-GFP and Erg6-mcherry, were grown at 30°C to either log phase or were depleted from glucose for 4 days. Changes in protein localizations were determined. Single plane images are shown. Bars: 2 µm. (B) Cells expressing Acc1-GFP/Pis1-3Xmcherry/Psd1-3Xmcherry/Erg6-mcherry were grown to log phase in SD medium at 30°C. Cells were washed twice with water and glucose depleted by transferring them to fresh SC medium. Cells were monitored for foci formation on different days by fluorescence microscopy. Time dependent sequestration of different proteins was quantified from multiple repetitions. Standard deviations are given.

2.8 Reversible spatial redistribution of ER and mitochondria upon glucose starvation

As ER and mitochondria localized lipid biosynthetic enzymes accumulated into punctate structures upon prolonged glucose starvation, I could envision two possibilities to explain this observation. One being that the lipid biosynthetic enzymes specifically accumulated into these punctate structures while the ER and mitochondrial spatial organization being unaffected. The other possibility being that ER and mitochondria themselves undergo spatial reorganization causing redistribution of their resident enzymes. To differentiate between the two possibilities, independent ER (Sec63-3xmcherry and ss-dsRed-HDEL stain nuclear and cortical ER; Rtn1-mcherry stains only cortical ER) and mitochondrial markers (Shm1-GFP) were analyzed. All the tested ER and mitochondrial markers showed accumulation into punctate structures similar to the enzymes (Pis1, Psd1) tested (Figure 2.11A/B). It should be noted that only the cortical ER redistributed after starvation while the nuclear ER remained largely unaffected (both for the tested enzymes and independent ER markers).

I next tested whether the global reorganization of ER and mitochondria is reversible upon addition of glucose. Indeed, punctate structures of ER (Rtn1) and mitochondria (Shm1, Psd1) markers, as well as ER- and mitochondria resident enzymes involved in lipid biosynthesis (Pis1) regained their normal spatial organization within 120 min upon glucose addition (Figure 2.11C-E).

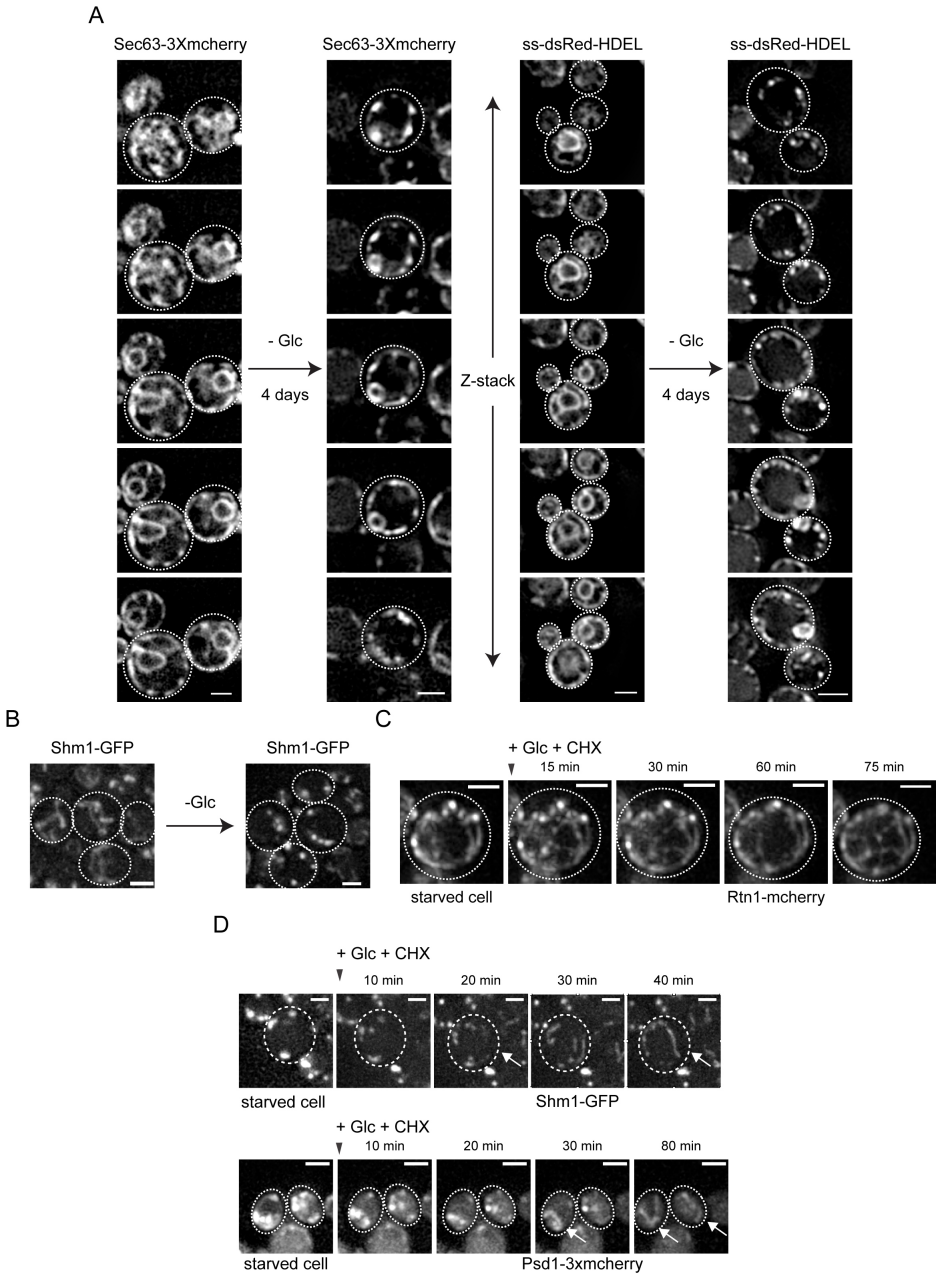

Figure 2.11: Reversible spatial re-distribution of ER and mitochondria upon glucose starvation.

(A) *S. cerevisiae* cells expressing the ER markers Sec63-3Xmcherry or ss-dsRed-HDEL were grown at 30°C to log phase or depleted of glucose (4 d). (B) *S. cerevisiae* cells expressing the mitochondrial marker Shm1-GFP were grown at 30°C to log phase or depleted of glucose (1 d). Glucose starved *S. cerevisiae* cells expressing the peripheral ER marker Rtn1-mcherry(C) or Shm1-GFP (D-upper panel) or Psd1-3Xmcherry (D-lower panel) were resuspended in PBS buffer containing 2% (w/v) glucose and cycloheximide (CHX). Changes in localization of respective proteins was recorded at the indicated timepoints.Bars: 2 µm.

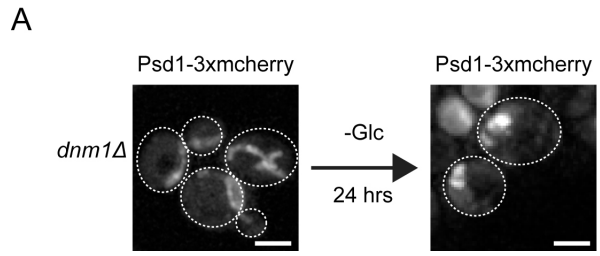

Figure 2.12: Fragmentation of mitochondria upon glucose depletion.

(A) Mitochondria continue to accumulate into punctate structures in mitochondrial fission defective strains. *dnm1Δ* cells (defective in mitochondrial fission) expressing Psd1-3Xmcherry were grown to log phase, washed twice with water and starved of glucose for 24 hrs. Psd1-3Xmcherry continued to accumulate into punctate structures upon glucose depletion.

Mitochondria are dynamic organelles that constantly change structure due to fission and fusion events. Increased mitochondrial fission has been described during stationary phase/upon nutrient limitation. I therefore monitored mitochondrial reorganization in in *dnm1Δ* cells, which are deficient in fission. Mitochondria still exhibited structural organizations in *dnm1Δ* cells upon glucose depletion (albeit with a fewer number of foci per cell), suggesting that fragmentation rather than fission of mitochondria leads to their punctate distribution (Figure 2.12A).

2.9 Glucose starvation induced ER and mitochondrial spatial redistribution correlate with changes in lipid profile

I wanted to test for a possible correlation in the observed sequestration of FAS and organellar reorganization upon glucose starvation with alterations in lipid profile. To my knowledge, this is the first time, such a detailed correlative lipidomic analysis has been performed under prolonged glucose starvation. Total lipids were extracted from cells starving of glucose at different time points (0 – 4 days) and analyzed both qualitatively (phospholipids, sphingolipids and ceramides) and quantitatively by a mass spectrometry based approach (Figure 2.13A-D). The data suggests that upon glucose starvation, there is regulation of glycerophospholipid and sphingolipid biosynthesis and turnover. Species-specific changes in phospholipids were observed. Total levels of phosphatidyl ethanolamine (PE) sharply dropped within one day of glucose depletion and phosphatidyl choline (PC) levels decreased continuously during the period of scarcity. In contrast, levels of phosphatidyl inositol (PI) increased upon glucose starvation, whereas levels of phosphatidyl serine (PS) remained unchanged (Figure 2.13A).

Levels of ceramides and sphingolipids also showed different alterations upon glucose depletion (Figure 2.13B-C). I do not see any obvious correlation between the timing of FAS foci onset and changes in lipid profile, leaving the trigger of FAS foci formation and the resulting physiological consequences unexplored. However, I notice a correlation between the onset of ER and mitochondrial spatial reconstruction upon glucose starvation with the drop in PC and PE levels (24 h) and an increase in PI levels. Similarly, ceramides, mannosyl inositol phoshoryl ceramide (MIPC) and Inositolphosphoryl- mannosyl inositol phosphoryl ceramide (MIP2C) levels drop within one day of glucose depletion. Thus global reorganizations of ER and mitochondria appear to affect phospholipid and sphingolipid levels. Whether changes in lipid levels are caused by differences in lipid biosynthesis, turnover or lipid flux between organelles awaits further analysis.

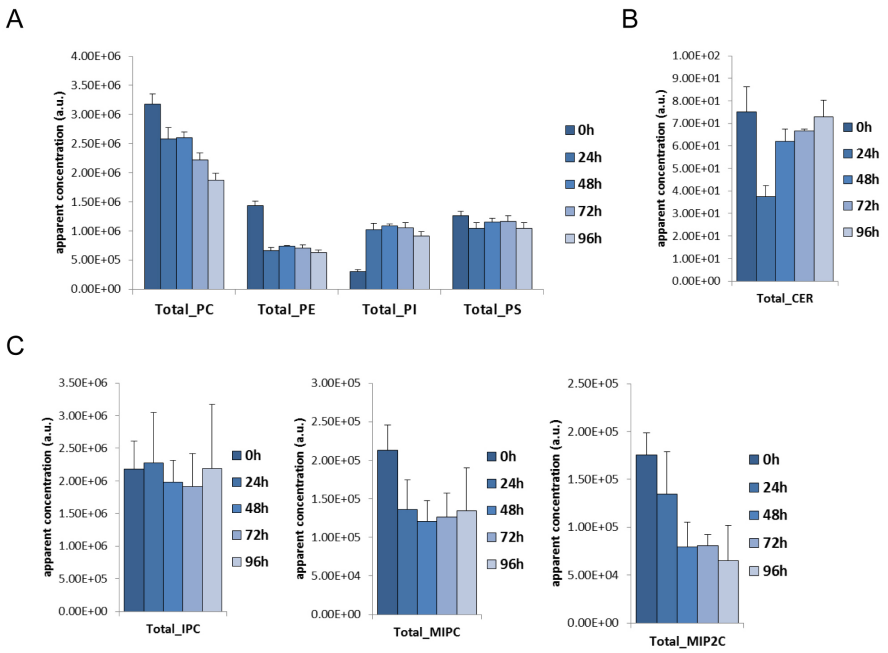

Figure 2.13: Qualitative and quantitative alterations in lipid profiles upon glucose depletion.

S.cerevisiae cells were grown at 30°C to log phase or starved from glucose. Total cell lysates were prepared at the indicated timepoints of glucose starvation and lipid compositions were analyzed by mass spectrometry. Changes in levels of different phospholipid species (A) and sphingholipids and ceramides (B) were determined. PC: Phosphatidyl choline; PE: Phosphatidyl ethanolamine; PS: Phosphatidyl serine; PI: Phosphatidyl inositol; IPC: Inositol phosphoryl ceramide; MIPC: Mannosyl inositol phoshoryl ceramide; MIP2C: Inositolphosphoryl- mannosyl inositol phosphoryl ceramide.

Taken together, this study distinguishes starvation-induced granules from misfolded protein aggregates and sheds light on the nature and possible physiological role of starvation induced sequestrations and thereby clarifying the existing controversy on starvation induced inclusions. Moreover, this study extends the known localization changes from cytosolic enzymes to entire organelles thereby extending our knowledge on metabolism driven organellar dynamics.

3 Discussion and outlook

Recently, there have been several reports for proteins accumulating into foci or rod shaped structures during conditions of nutrient depletion [66, 51, 53, 52, 50, 67]. Like classical heat induced protein aggregates, some of the starvation-induced sequestrations require Hsp42 for their formation[10, 13]. Additionally, several chaperones such as Hsp42 and Hsp104 that are known to aid in protein disaggregation accumulate into punctate structures during starvation conditions [53]. A proteome wide analysis [59] claimed many of these sequestrations including Gln1 to represent protein aggregates based on the following: 1) a partial overlap in the set of proteins known to form sequestrations during starvation with those that aggregate under conditions of known proteotoxic stress; 2) Co-localisation of these sequestrations with chaperones such as Hsp82.

In contrary, given that many of these sequestrations can be reversed by addition of specific metabolites [66, 51, 53, 52, 50, 67], there have been proposals supporting these sequestrations to represent storage assemblies. Further, co-sequestration of functionally related proteins such as Ura7 and Ura8 as well as purine biosynthetic enzymes in mammalian cells have been reported [52, 50]. Co-sequestration of proteins is believed to aid in substrate channeling and thereby aiding in efficient biosynthesis. In the light of such opposing suggestions made, the nature of these sequestrations and their relationship to classical protein aggregates remains unresolved.

Given that Fatty acid synthetase (FAS) subunits sequester under conditions of both proteotoxic and metabolic stress [68, 69, 53], I use Fas1/2 - subunits of FAS as a model substrate for a systematic study addressing the above mentioned discrepancies.

I find that both subunits of FAS, Fas1/2, co-sequester into one or more foci under conditions of metabolic stress (stationary phase or prolonged glucose starvation) (Fig.1.1A). Further, I find that FAS foci do not represent classical protein aggregates as: 1) FAS foci do not co-localise with Hsp104 (Fig.1.3A) 2) FAS foci are dynamic and reversible upon addition of glucose in an Hsp104 independent manner (Fig.1.3D-E) and 3) FAS foci exhibit enzymatic activity (Fig.1.9A-B).

Accordingly, the starvation-induced deposits of all tested proteins were unique and did not intermix (Fig.1.1C), suggesting that sequestrations of distinct proteins follow specific pathways but are not caused by misfolding, which should lead to co-aggregation. Moreover, like FAS, Gln1-mcherry foci do not co-localise with Hsp104 and are resolubilised in an Hsp104 independent mechanism upon addition of glucose indicating these foci not to be classical protein aggregates (Fig.1.4A-B). This

observation is consistent with a recent study [70] where Gln1-mcherry rods formed in advanced starvation state were proposed to represent storage assembly of the enzyme.

Put together, nutrient limitation does not seem to globally affect protein folding and to induce aggregation of a wide variety of metabolic enzymes as recently suggested [59].

Given that FAS foci are not protein aggregates, one could envision two different possible reasons for FAS sequestrations: 1) Localized active synthesis of fatty acids and/or phospholipids or 2) Restrict the distribution and hence the availability of FAS in the cytosol to limit utilization of its substrate, acetyl-coA, which could then be channelized for other essential metabolic pathways under starvation.

In order to explore the first possibility, I studied the changes in localization of other enzymes involved in lipid biosynthesis. In this regard, I do not observe co-localization of FAS foci with enzymes either delivering FAS substrates (Acc1) or using FAS generated products for lipid biosynthesis (Pis1, Psd1, Erg6), although all these enzymes exhibit spatial reorganization upon starvation (Fig.1.10A). The specific, non-mixing sequestrations of enzymes tested rather supports a role of FAS foci as reversible storage compartments. Similarly, starvation-induced Gln1 rods have been recently suggested to represent storage compartments, exhibiting reduced enzymatic activity [70]. Therefore, in support of the second possibility, I speculate that FAS sequestrations while retaining enzymatic activity, might lower utilization of the central metabolite acetyl-CoA required for fatty acid synthesis in cells by restricting the local availability of FAS. Upon addition of glucose, availability of FAS is restored rapidly for efficient fatty acid synthesis and subsequent resume of growth.

The precise trigger/s for FAS sequestration remains unknown and needs further exploration. Proteasome storage granules (PSGs) and Gln1 rod formation were recently suggested to be triggered by changes in intracellular pH under nutrient limiting conditions [71, 70]. Given that FAS sequesters at a much later time frame during starvation as compared to PSGs and Gln1 rod formation (Fig.1.1D)[70], pH change is unlikely to be the trigger for FAS sequestration.

Cells counteract lipid disequilibrium via reorganizing their proteome [72]. Thus it is possible that FAS sequestration could be triggered by changes in lipid equilibrium. Using mutants defective in different stages of secretory pathway, lipid disequilibrium was induced and faster kinetics of FAS sequestration was observed (Fig.1.7), thus supporting the possibility of alterations in lipid equilibrium as a possible trigger for FAS sequestration. However, no obvious correlation could be drawn between FAS foci formation and observed changes in total lipid levels during starvation (Fig.1.13).

Metabolic status rather than cell cycle signals have been implicated to induce protein sequestrations during quiescence [55]. To explore the possibility of metabolic status to trigger FAS sequestrations some of the key nutrient sensing pathways such as Snf1 and TOR signaling were mis-regulated using well characterized mutants of the pathways. Deregulation of the pathways affected the rate of FAS sequestration,

indicating that metabolic status could also indeed be a possible trigger for FAS sequestration (Fig.1.5). A correlative metabolomic study could give further insights into possible regulation of FAS sequestration by specific metabolites such as its substrate, acetyl-coA.

Ssb, a ribosome-associated Hsp70 chaperone is known to negatively regulate Snf1 activity status {von Plehwe, 2009 #53}. While similar to the hyperactive Snf1 status in *reg1Δ* cells, *ssbΔ (ssb1Δssb2Δ)* cells exhibit faster kinetics of FAS sequestration, which are however independent of Snf1 given that *ssbΔsnf1Δ* cells continue to sequester FAS at similar kinetics (Fig.1.6). Additionally, another ribosome associated chaperone mutant, namely, *nacΔ* (*bbt1Δegd1Δegd2Δ*) exhibits similar phenotypes. Additionally, unlike wild type cells with one FAS focus, *ssbΔ* and *nacΔ* cells harbor multiple FAS sequestrations. Thus, ribosome associated chaperones affect FAS sequestration. Future work will shed more light on their role in regulating protein sequestrations.

I also observe that ER and mitochondria resident enzymes of lipid biosynthesis form punctate structures upon glucose depletion. These relocalizations are caused by global spatial reorganizations of ER and mitochondria, which are entirely reversible and can be rapidly reverted by glucose addition (Fig.1.11A-D). Our findings extend the known starvation-induced localization changes from individual enzymes to entire organelles. Interestingly, changes in observed ER and mitochondria morphology correlate with changes in levels of specific lipids (Fig.1.13). Decrease in PC and PE levels could be caused by defects in shuttling of PS from ER to mitochondria. In support of such possibility, yeast cells lacking the ERMES (ER-mitochondria encounter sites) complex (*mdm34Δ*) and having an altered ER structure due to mutations in ER-shaping proteins (*rtn1Δ yop1Δ*) exhibit defects in PS shuttling that correlates with reduced PE steady state levels [64].

Notably, the ER exit marker Sec16 also reversibly accumulate into dense punctate structures in Drosophila cells upon depletion of serum and amino acids [56], however, the physiological relevance of the observed changes are unknown. Also, mitochondrial fragmentation in response to glucose depletion, resembling our observation, has been reported for mammalian cells [57]. While the precise reason and the molecular machineries involved in mitochondrial fragmentation upon glucose depletion remains unknown, depletion of amino acids together with serum and glucose induces a strong elongation and tubulation of mitochondrial network. Tubulated elongated mitochondrial network are more stable and resist degradation via autophagy. Furthermore, addition of glucose, amino acids and serum reversed the mitochondrial tubulation [57]. Therefore, reversible organellar reorganization seems to be a common theme in adaptation of cells to starvation.

In summary, while my work sheds light on the nature of starvation-induced FAS sequestration and distinguishes it from classical protein aggregates, the possible role of ribosome associated chaperones (Ssb, NAC) in regulating FAS sequestration needs to be further analysed. Moreover, while the metabolic status is governing FAS sequestration, correlative metabolomic analysis could aid in deciphering the levels of key metabolites whose changes could then govern FAS sequestration. Furthermore,

it could aid in understanding the physiological function of FAS sequestration.

While a good correlation is observed between the changes in phospholipid species and ER- mitochondrial reorganisation upon glucose starvation, the link needs to be further explored to gain insights into the trigger for the observed organellar spatial re-organisations and perhaps their physiological relevance. The molecular machineries governing these organellar changes also need to be deciphered. Given that the phenomenon is conserved in humans, as well, their understanding would likely contribute in expanding our repertoire of knowledge for advancing medicine.

4 Materials and methods

4.1 Materials

4.1.1 Chemicals

All used chemicals were purchased from Roth, Sigma-Aldrich, Fluka, Roche, Invitrogen or AppliChem.

4.1.2 Technical equipment

Table 4.1: Technical equipment.

Item	Manufacturer
Agarose gel chambers and trays	ZMBH workshop
Balances	Mettler
Benchtop robot ROTOR HDA	Singer Instruments
Bioanalyzer	Agilent Technologies
Centrifuges	Sorvall, Eppendorf, Heraeus
Glass ware	Schott
Gradient Master	Biocomp
Gradient Station	Biocomp
Incubators	Heraeus
Lumat, LB9501	Berthold Technologies
Nanodrop 2000	Thermo Scientific
PCR machine, T-Gradient	Biometra
Phosphoimager FLA-3000	Fujiifilm
Photometer, Specord 205	Analytik Jena
MaxQ 7000 water bath	Thermo Scientific
Mixer mill MM 400	Retsch
Manuel pipetting system Liquidator™ 96	Mettler
Power supply	Perkin-Elmer, ZMBH workshop
SDS gel chambers	Biorad
Vortex mixer	Neolab
Western blot chambers, semi-dry	Biorad

Table 4.2: Expendable items.

Item	Manufacturer
Cover slides	Greiner
Cuvettes	Sarstedt
Falcon tubes 15, 50 ml	Greiner
Glass bottom dishes	MatTek Corp
Microcentrifuge tubes	Eppendorf
Object slides	Roth
Plastic tubes 1.5, 2 ml	Sarstedt
PVDF membrane, Roti-PVDF	Roth
Sterile filters	Millipore
Whatman paper, 3 mm	Schleicher &Schuell

Table 4.3: Microscopy systems.

Microscopy system	Location
Olympus xcellence PointFRAP IX81 microscope	ZMBH Imaging Facility/Bukau Lab
Olympus xcellence TIRF/Scanner FRAP IX81 microscope	ZMBH Imaging Facility
Zeiss LSM 780	ZMBH Imaging Facility

Table 4.4: Kits.

Kit	Source
Plasmid Midi/Maxi Kit	Qiagen
MiniElute PCR Purification Kit	Qiagen
QIAprep Spin Miniprep Kit	Qiagen
Z-competent E. coli Transformation Buffer Set	Zymoresearch
ZyppyTM Plasmid Miniprep Kit	Zymoresearch
Zymoclean DNA Gel Recovery Kit	Zymoresearch

All kits and reagents were used according to the manufacturer's protocol unless otherwise stated.

Table 4.5: Enzymes.

Enzyme	Source
T4-DNA ligase	Lab collection
Phusion High Fidelity DNA polymerase	Lab collection
Restriction enzymes	NEB, Fermentas

Table 4.6: DNA and protein size standards.

Size standard	Source
GeneRuler DNA Ladders	Thermo Scientific
Prestained protein weight marker #671	Thermo Scientific

Table 4.7: Antibodies.

Antibody	Species	Source
α-Myc	mouse	sigma
Alexa 488	goat	Life Technologies
α-FAS	rabbit	Life Technologies
α-YFP	rabbit	Lab collection

Table 4.8: Software.

Software	Company
Adobe Acrobat	Adobe
Adobe Illustrator9.0	Adobe
Adobe Photoshop	Adobe
ImageJ	NIH
Image Reader	Fujifilm
Microsoft Office	Microsoft
Papers	Mekentosj
Excel	Microsoft
Xcellence	Olympus
ZEN (2010)	Carl Zeiss

4.2 Methods

4.2.1 DNA work

4.2.1.1 PCR

10x Phusion buffer

100 mM Tris pH 8.8

500 mM KCl
20 mM $MgSO_4$
1% Triton X-100

PCR reaction mix	Volume [µl]
10x Phusion buffer	10
10 mM dNTPs	2
10 µM primer #1	2
10 µM primer #2	2
DNA template	0.5-1
adH_2O	100

For amplification of the DNA fragment of interest, a PCR reaction was performed using following protocol:

Temperature [°C]	**Time [min]**	**Cycles**
98	5	1
98	0.5	34
according to primers (50-63)	0.5	
72	according to PCR product (15 s/1 kb)	
72	3	1
16	∞	1

4.2.1.2 Restriction digest

1U restriction enzyme was used to digest 1 µg of DNA within 1 hour. Reaction conditions and enzyme concentrations were used according to the manufacturer's instructions.

4.2.1.3 Agarose gel electrophoresis

10x TBE buffer	**6x DNA loading dye**
0.9 M Tris pH 8.0	40% sucrose
1.2 M boric acid	0.2% Orange G
20 mM EDTA	

0.8-2% agarose gels were prepared by boiling agarose in 0.5x TBE buffer until completely dissolved. Ethidium bromide was added to the molten agarose and poured in a flat-bed tray with combs. DNA samples in DNA loading buffer were loaded on the gel and separated in an electrical field. The gel was analyzed under a UV-light tray at 265 nm. Gel excision was performed at less intense UV-light at 365 nm to avoid DNA damage.

4.2.1.4 Ligation

2x Rapid ligation buffer	**10x Ligation buffer**
132 mM Tris pH 7.6	500 mM Tris pH 7.6
20 mM $MgCl_2$	100 mM $MgCl_2$
2 mM DTT	100 mM DTT
2 mM ATP	10 mM ATP
15% PEG 6000	15% PEG 6000

Ligation was performed either in the rapid or in the regular ligation buffer. DNA fragments were mixed in the ligation buffer, incubated at 14°C for 1 hour and transformed into competent *E.coli* cells.

4.2.2 Protein analysis

4.2.2.1 Bradford assay

The Bradford reagent (Biorad) was diluted 1:5 with water and 1 ml of the reagent was mixed with 1-5µl of the protein solution (BSA protein standard or protein sample). The absorption was measured at 595nm in a photo spectrometer. Protein concentrations were calculated from the BSA standard curve.

4.2.2.2 SDS-PAGE

For SDS Page the Criterion™precast gel system (Biorad) was used .The procedure was performed according to the manufacturer's instructions.

4.2.2.3 Western blotting

10x TBS	**10x TBST**	**Blocking buffer**
1 M Tris/HCl pH 8.0	1 M Tris/HCl pH 8.0	3% BSA in TBST
1.5 M NaCl	1.5 M NaCl	
	0.05% Tween-20	

Western Blot experiments were done using the Trans-Blot® Turbo™ Transfer System (Biorad) according the manufacturer's instructions. PVDF membranes

were then blocked in blocking buffer for 45 min. Incubation with the primary antibody diluted in blocking buffer was done for 2 hrs at RT. Subsequently the membrane was washed three times for 10 min with TBST followed by incubation with alkaline phophatase-coupled secondary antibody at RT for 45 min. After three more washing steps with TBST and one washing step with TBS the membrane was incubated with ECF substrate, which can be dephosphorylated by alkaline phosphatase producing a fluorescent product. Fluorescent bands were detected at the Phosphoimager FLA-3000.

4.2.3 Bacterial work

4.2.3.1 Growth conditions

LB medium	**SOC medium**
1% tryptone	20% tryptone
0.5% yeast extract	20% 5x amino acid mix
0.5% NaCl	2% glucose

E.coli cells were grown in LB medium at 30 or 37°C under constant shaking in the presence of antibiotics.

4.2.3.2 Preparation of competent *E.coli* cells

Z-competent E.coli cells were prepared either using Z-Competent™ *E. Coli* Transformation Kit (ZYMO RESEARCH) according to manufacture's protocol or the $CaCl_2$ method. For the $CaCl_2$ method, 50 ml *E.coli* XL1 Blue or Δ*clpB* MC4100 cells were grown in LB medium to mid-logarithmic growth phase at 30°C and briefly incubated on ice. Subsequently cells were washed once with 20 ml 100 mM $MgCl_2$, once with 20 ml 100mM $CaCl_2$, resuspended in 4 ml 100mM $CaCl_2$ and incubated for up to 4 hrs on ice. Glycerol was added to a final concentration of 10%, cells were shock-frozen in liquid nitrogen and stored in aliquots at -80°C.

4.2.3.3 Transformation of *E.coli* cells

An aliquot of competent *E.coli* cells was thawed on ice and DNA was added. This mixture was incubated for 20 min on ice with occasional mixing. Cells were incubated at 42°C for 1 min, chilled briefly on ice and incubated for 45 min at 37°C in LB medium prior to plating on antibiotics containing LB plates. In the case of ampicillin resistance transformed cells were directly plated on selective plates and incubated at 37°C overnight.

4.2.4 Yeast work

4.2.4.1 Yeast strains, media and growth conditions

mcherry and GFP tagged chromosomal constructs or gene knockouts were created using optimized PCR-amplified cassettes (Janke et.al, 2004). Supplementary Table 1 lists all strains used in this study, Supplementary Table 2 includes all used plasmids. Synthetic medium (SD medium- 6.7 g/l of Yeast Nitrogenous bases without amino acids, 0.79 g/l of amino acid dropouts and 2 % (w/v) glucose) was used for cell growth. To starve cells of glucose, cells were washed twice with water and transferred to SC medium lacking glucose (6.7 g/l of Yeast Nitrogenous bases without amino acids, 0.79 g/l of amino acid dropouts). Cells were grown in SD medium at 30°C on a shaking incubator at 150 rpm. To test the behavior of protein sequestrations upon replenishment of nutrients, stationary phase or glucose depleted cells were harvested by centrifugation, resuspended in either SD medium or SC medium or PBS buffer with or without glucose (2% (w/v)). In all the cases, cycloheximide was added to a final concentration of 100 µg/ml. In some experiments 3 mM guanidiniume hydrochloride (GdnHCl) was added to inhibit Hsp104 activity.

4.2.4.2 Transformation of Yeast Cells

10 ml yeast cells were grown in YPD to OD_{600} 0.3-0.6, pelleted at 3,000 rpm for 2 min and washed once in 10 ml lithium-acetate mix and used for one transformation. The transformation mix was incubated in an eppendorf tube on a wheel at RT for 30 min. The heat shock was performed at 42°C for 10-15 min, followed by a centrifugation step at 3,000 rpm for 2 min and washing with YPD medium. Cells were transferred into a glass tube, incubated in YPD on the wheel overnight at RT to acquire antibiotic resistance if necessary and plated on the respective antibiotic plate. For auxotrophic markers cells were directly plated on the respective drop-out plate. Clones were analyzed by microscopy, colony PCR and/or western blotting after 2-3 days of growth at 30°C.

4.2.4.3 Extraction of Genomic DNA from Yeast

DNA extraction buffer	**$T_{10}E_1$ buffer**
10 mM Tris pH 8	40% polyethylen glycol
100 mM NaCl	100 mM lithium acetate
1 mM EDTA	10 mM Tris
1% SDS	1 mM EDTA
0.2% Triton X-100	

Genomic DNA was extracted as described by *Hoffman and Winston* [**?**]. Yeast cells were transferred from the plate into 200 µl of DNA extraction buffer in glass tubes. After the addition of 500 µl of acid-washed glass beads (425-600 µm, Sigma) and 200 µl of 1:1 phenol:chloroform mix, cells were vortexed at full speed for 4 min. 200 µl $T_{10}E_1$ buffer was added to the lysate followed by vortexing for 30 s at full speed. The lysate was transferred into an eppendorf tube and centrifuged at 12,000 rpm for 10 min at RT. 300 µl of the supernatant was removed, transferred into a clean tube containing 750 µl ethanol and mixed. The DNA was collected by centrifugation at 12,000 rpm for 10 min and the supernatant was removed. The pellet was dried, resuspended in 40 µl dH_2O and stored at -20°C.

4.2.4.4 Yeast Colony PCR

10x Taq buffer
200 mM Tris pH 8.8
100 mM $(NH_4)_2SO_4$
100 mM KCl
20 mM $MgSO_4$
1% Triton X-100

Colony PCR reaction mix	Volume [µl]
10x Taq buffer	2.5
10 mM dNTPs	0.5
10 µM primer #1	0.75
10 µM primer #2	0.75
adH_2O	24.5
+ Taq polymerase (hot start)	0.5

The primers for colony PCR were chosen to give a product of maximum 1000 bp to ensure the presence of the corresponding DNA fragment in the cell lysate or in the preparation of the genomic DNA. Usually, yeast cells were directly taken from the agar plate, resuspended in 24.5 µl of the reaction mix and boiled at 99°C for 10 min to release the DNA. Taq polymerase (Bukau Lab stock) was added to each tube, mixed and used for PCR. Following protocol was used:

Temperature [°C]	**Time [min]**	**Cycles**
94	5	1
94	0.5	34
according to primer (50-63)	0.5	
72	according to PCR product (1 min/1 kb)	
72	10	1
16	∞	1

The resulting PCR product was analyzed on a 1% agarose gel and documented

4.2.4.5 Anchor-away and viability assays

Cells co-expressing Pma1-FKBP12 and Fas2-mcherry with either Fas1-FRB or untagged Fas1 were glucose depleted as described. Either DMSO or rapamycin (1µg/ml) was added to the cells immediately after glucose starvation. Localisation of Fas2-mcherry was monitored within minutes to ensure that rapamycin treatment led to anchoring away of FAS. Subsequently, aliquots of cultures were taken on different days of starvation and viability measured by two methods: 1) cell cultures were adjusted to identical OD600 values, diluted fivefold and spotted onto YPD and YPD + rapamycin (10 µg/ml final). The viability of cells was monitored by determining the plating efficiency of cells incubated for 2 days at 30°CC. 2) 1 OD600 of cells were harvested and resuspended in PBS buffer. A 5 mM Sytox green solution (Invitrogen) was used to stain cells at 10,000 times dilution for 10 min at room temperature. The cells were harvested by centrifugation, washed in PBS and immediately analysed by FACS (BD FACS CantoTM II) using a 488 nm laser. A total of 20,000 events were measured at each time point per repetition. Dead cells being stained by the dye can be separated and thus the percentage of viable cells calculated.

4.2.4.6 Image acquisition, processing, and data analysis

Cells were treated as indicated, harvested by centrifugation and resuspended in PBS. Optical sections of 0.2 µm were acquired to image the whole cell volume using a widefield system (xcellence IX81, Olympus) equipped with a Plan-Apochromat 100x /NA 1.45 oil immersion objective and an EMCCD camera (Hamamatsu ORCA-R2 or Hamamatsu ImagEM Enhanced (C9100-13) or Hamamatsu EM-CCD (C9100-02). Acquired z-stacks were deconvolved

with xcellence software using the Wiener Filter. All further processing of digital images was performed with ImageJ. Time lapse microscopy For sample preparation a round bottom dish was coated with concanavalin A (ConA). Cells were adhered on the ConA coated coverslip for 15 min, unbound cells were removed by washing and a final volume of 3 ml of PBS buffer containing 2 % (w/v) glucose and 100 µg/ml of cycloheximide was added. Image acquisition was started simultaneously and images were acquired using the xcellence IX61 microscope using a Plan-Apochromat 100x/NA 1.45 oil immersion objective including hardware autofocusing during the course of the experiment. Fourteen optical sections of 0.2 µm were acquired to image the whole cell volume. Stacks were deconvolved as described.

4.2.4.7 Immunofluorescence

For immunostaining cells were fixed with 4% (v/v) p-formaldehyde/100mM KPi (Sigma Aldrich) for 1 h prior to cell wall digestion with 500 µg/ml Zymolase T-100 in wash buffer (1.2 M Sorbitol/100 mM KPi pH 6.5) supplemented with 20 mM β-mercaptoethanol at 30°C. Spheroblasts were attached to poly-Lysine coated cover slides, permeabilized by washing three times with 1% Triton X-100/100 mM KPi pH6.4 and blocked for 1 h with 1% (w/v) BSA in 100 mM KPi pH6.4. Mouse anti-myc antibody (clone 9E10) at a dilution of 1:500 in blocking buffer was applied to spheroplasts, incubated for 2 h at room temperature. Spheroplats were rinsed in blocking buffer three times. AlexaFluor® 488 Goat Anti-Mouse IgG (H+L) secondary antibody (Invitrogen) was applied and incubated at room temperature for 1 h. Following secondary antibody incubation, spheroblasts were stained embedded in 55% glycerol.

4.2.4.8 Fluorescence loss in photobleaching

(FLIP) measurements For FLIP analysis, cells were grown to stationary phase phase, immobilized on concanavalin-A coated glass-bottom culture dishes. FLIP measurements were performed at 25°C for 20 individual cells. A defined area was bleached 27 times for 380 s. Laser intensities for bleaching were set to 100% for the 561 nm laser. Laser settings for imaging was set to 3% for the 561 nm laser. Measurements were performed at 25°C on a confocal microscope (LSM 780; Carl Zeiss) equipped with a 63x/1.40 NA oil objective lens and 561-nm laser lines for mcherry image acquisition and photobleaching. The resulting loss of fluorescence in the region of interest as a function of time provides a measure of the relative exchange rate with the bleached cytoplasmic fraction of molecules. Quantification of FLIP experiments was performed using ZEN 2010 software (Carl Zeiss). The fluorescence intensity of the background (Fbg), the region of interest (ROI) at a particular time point (Ft),

and the fluorescence intensity before the first bleach (F0) was determined. To calculate the loss of fluorescence at a particular time point, the formula (Ft - Fbg)/(F0 - Fbg) ° X 100 was used. Curves represent the mean of 20 cells and the corresponding standard error.

4.2.4.9 Correlative Fluorescence microscopy and electron tomography

Sample preparation, data acquisition and the correlation procedure were essentially done as described before (Kukulski, Schorb et al. 2011, Kukulski, Schorb et al. 2012), with minor modifications. Cultures grown under starvation conditions and, in parallel, to log phase, of yeast cells expressing Fas1-mCherry, Sec63-GFP, were pelleted by vacuum filtration (McDonald 2007), loaded into aluminum planchettes 0.1/0.2 mm, covered with the flat side of aluminum planchettes 0.3 mm (M. Wohlwend, Sennwald, CH) and cryo-fixed using a BAL-TEC HPM-010 high pressure freezer. Samples were freeze-substituted with 0.1% uranyl acetate in acetone, embedded in Lowicryl HM20 resin and sectioned according to the protocol published before (Kukulski, Schorb et al. 2011). EM grids with 320 nm resin sections were incubated section-face down for 10 minutes on 15 µl drops of 50 nm TetraSpeck microspheres (Life Technologies, Carlsbad, CA, USA) diluted 100 x in phosphate-buffered saline (PBS), washed with water and blotted 3 times. For fluorescence microscopy, EM grids were placed between two coverslips in a layer of water, as depicted in (Kukulski, Schorb et al. 2012). Imaging was done on an Olympus IX81 microscope with a 100x NA1.45 objective and an Orca-ER camera (Hamamatsu). An X-Cite 120 PC lamp (EXFO) was used for fluorescence imaging. Excitation filters for GFP, mCherry and blue channel were 470/22 nm, 556/20 nm and 377/50 nm. Emission filters were 520/35 nm, 624/40 nm and 520/35 nm, respectively. The blue channel was recorded for distinguishing the TetraSpeck from colocalizing GFP and mCherry signals. 15 nm Protein A-coupled gold beads were adhered to both faces of the grids as fiducial markers for tomographic reconstructions and sections were stained with Reynolds lead citrate for 15 minutes. Electron tomographic tilt series were acquired using SerialEM software (Mastronarde 2005) on a FEI TF30 microscope operated at 300 kV and equipped with a FEI 4k Eagle CCD camera, using a dual-axis tomography holder (Fischione Model 2040). Dual-axis tilt series were acquired from -60 to 60° at 1° increment and 1.18 nm pixel size. For fiducial-based correlation, lower magnification single-axis tilt series were acquired from -60 to 60° at 3° increment and 2.53 nm pixel size. The IMOD software was used for tomogram reconstruction (Kremer, Mastronarde et al. 1996). For location of fluorescent signals in electron tomograms, the correlation procedure described in (Kukulski, Schorb et al. 2012) was applied. In brief, virtual slices in which TetraSpeck microspheres on the section surface were visible were selected from

the low mag tomogram and averaged using ImageJ (http://imagej.nih.gov/ij). Centroids of TetraSpeck signals in the same channel as the fluorescent signal of interest (RFP for Fas1-mCherry) were determined with sub-pixel accuracy and assigned to the corresponding positions in the averaged EM image using the MATLAB Control Point Selection Tool. Using TetraSpeck microspheres as fiducial markers permitted to correlate directly to the fluorescent image of interest, avoiding the need to correct for drift between fluorescent images. The transform between fluorescence and electron microscopy images was determined based on the pairs of coordinates, and was used to map the sub-pixel fitted centroid of the fluorescent spot of interest onto the low mag electron tomogram. In a second step, the coordinates of the predicted fluorescent spot position were transformed to the high magnification tomogram in an analogous procedure based on the 15 nm gold beads.

4.2.4.10 Tokuyasu Immuno-electron microscopy

Cells expressing Fas1-mcherry, Sec63-GFP were either grown to log phase or glucose starved for 4 days. Cells were then chemically fixed, treated with periodic acid, gelatin embedded, sucrose infiltrated, cryo-sectioned and immune-labelled as described in Griffith et al, 2009. While α – FAS antibody (rabbit) at 1:30 dilution was used as primary antibody, anti-rabbit antibody charged with 10 nm gold particles were used as secondary antibody. Sections were treated with 3 % Uranyl Acetate and dried. Images were acquired using FEI Tecnai G2 200kV Transmission Electron microscope.

4.2.4.11 Protein solubility and FAS activity assay

Log phase or glucose depleted yeast cells were harvested by centrifugation, resuspended in 50 mM Tris/HCl, 500 mM NaCl pH 8.5 supplemented with protease inhibitors (1 mM phenylmethylsulfonfluoride (PMSF), 5 µg/ml leupeptin, 10 µg/ml pepstatin, 8 µg/ml aprotinin, Proteaseinhibitor Mix FY (Serva)) and flash frozen in liquid nitrogen prior to pulverization by repeated mixer milling (MM 400 (Retsch), 30 Hz, 2 min). Cell lysates were pre-cleared by centrifugation at 3.000 x g for 5 min and total protein concentration of supernatants was measured by Bradford (Biorad) before separating soluble and insoluble fractions by centrifugation at 16.000 g for 20 min. The soluble fraction was removed and its protein concentration measured while the pellets were washed once with 50 mM Tris/HCl 150 mM NaCl pH 8.5 supplemented with protease inhibitors, centrifuged at 16.000 x g for 20 min and resuspended in 50 mM Tris/HCl, 500 mM NaCl, 8 M urea, 2% (w/v) SDS, 2 mM DTT pH 8.5 supplemented with protease inhibitors. SDS-PAGE and western blotting

with anti-YFP antisera analyzed distribution of Fas1-GFP to soluble or insoluble fractions. To determine FAS activity total lysates and supernatants of log phase and glucose depleted cells were added to 700 µl of FAS activity buffer (0.1 M Potassium phosphate buffer pH 6.5, 2.5 mM EDTA, 10 mM Cysteine, 0.3 mg/ml BSA, 0.24 mM acetyl coenzyme A, 0.15 mM NADPH) and activity was measured by addition of malonyl-CoA (0.28 mM) using conversion of NADPH to NADP at 340 nm as a readout using a spectrophotometer (Shimadzu UV-1601). 20 µM cerulenin, a specific inhibitor of FAS used to monitor specificity of the activity measured.

4.2.4.12 Lipidomics

Lipids were extracted and analyzed by mass spectrometry as described (Santos, Riezman et al. 2014). Briefly, 25 OD of cells were resuspended in 1.5 ml of extraction solvent [ethanol, water, diethyl ether, pyridine, and 4.2 N ammonium hydroxide (15:15:5:1:0.018, v/v)]. A mixture of internal standards (7.5 nmol 17:0/14:1 PC, 7.5 nmol 17:0/14:1 PE, 6.0 nmol 17:0/14:1 PI, 4.0 nmol 17:0/14:1 PS, 1.2 nmol C17:0-ceramide and 2.0 nmol C8-glucosylceramide) and 250µl of glass beads were added, the sample was vortexed vigorously (Multitube vortexer, Lab-tek International Ltd, Christchurch, New Zealand) for 5 min and incubated at 60°C for 20 min. Cell debris was pelleted by centrifugation at 1800xg for 5 min and the supernatant was collected. The extraction was repeated once and the supernatants were combined and dried under a stream of nitrogen or under vacuum in a Centrivap (Labconco Corporation, Kansas City, MO, USA). Half of the sample was used for ceramide and complex sphingolipids analysis, where we performed an extra step to deacylate glycerophospholipids using monomethylamine reagent [methanol, water, n-butanol, methylamine solution (4:3:1:5, v/v)](Cheng, Park et al. 2001). For desalting, both lipid extracts are resuspended in 300µl of water-saturated butanol and sonicated for 5 min. 150µl of LC-MS grade water was added, samples were vortexed and centrifuged at 3200xg for 10 min to induce phase separation. The upper phase was collected and the process was repeated twice. The combined upper phases were dried and kept at -80°C until analysis. For glycerophospholipid and sphingolipid analysis by ESI-MS/MS, extracts were resuspended in 500µl of chloroform:methanol (1:1, v/v) and diluted in chloroform:methanol:water (2:7:1, v/v/v) and chloroform:methanol (1:2, v/v) containing 5 mM ammonium acetate for positive and negative mode, respectively. A Triversa Nanomate® (Advion, Ithaca, NY, USA) was used to infuse samples with a gas pressure of 30 psi and a spray voltage of 1.2 kV on a TSQ Vantage (ThermoFisher Scientific, Waltham, MA, USA). The mass spectrometer was operated with a spray voltage of 3.5 kV in positive mode and 3 kV in negative mode. The capillary temperature was set to 190°C. Multiple-reaction

monitoring mass-spectrometry (MRM-MS) was used to identify and quantify lipid species (Guan, Riezman et al. 2010). Data was converted and quantified relative to standard curves of internal standards, which have been spiked in prior to extraction. Values are averages +/- standard deviation of three independent samples.

Acknowledgments

I thank Prof. Dr.Bernd Bukau for providing me a great opportunity to work in his laboratory. I am greatful for his supervision, kindness and constant support.

I thank PD Dr.Axel Mogk for his kindness, dedicated supervision and constant support.

I thank Dr.Brian Luke for his excellent scientific discussions, genuine interest, words of optimism and constant support.

I thank PD Dr.Tobias Dick for being my TAC member and for his constructive discussions.

I thank Dr.Holger Lorenz at the ZMBH Imaging facility for his constant support and guidance with microscopy.

I thank Dr.Aline Santos, Prof.Howard Riezman, Dr.Wanda Kukulski and Dr.John Briggs for fruitful collaborations.

I would like to thank Valeria, Ronny,Yuki, Frank, Josef and Lena for being wonderful colleagues and great friends. I thank all the members of Bukau lab for a great working experience.

I thank my parents and brother for all their support and blessings without which this work wouldn't have been possible.

I thank my friends Rajesh, Sahil, Sumit, Sowmya and Sanchari for making life in Heidelberg enjoyable.

Lastly, I thank the almighty for everything.

Bibliography

[1] **Hartl, F. U., Bracher, A.** and **Hayer-Hartl, M.**, *Molecular chaperones in protein folding and proteostasis*, Nature, Vol. 475, No. 7356, pp. 324–332, Jul 2011.

[2] **Yujin E Kim, Mark S Hipp, A. B. M. H. H. K. M. S. H. A. B. M. H. H.** and **Hartl, F. U.**, *Molecular Chaperone Functions in Protein Folding and Proteostasis*, Annual Review of Biochemistry, 2013.

[3] **Onuchic, J. N.** and **Wolynes, P. G.**, *Theory of protein folding*, Current Opinion in Structural Biology, 2004.

[4] **Chiti, F.** and **Dobson, C. M.**, *Protein Misfolding and Functional Amyloid and Human Disease*, *The Annual Review of Biochemistry*, 2006.

[5] **Eisenberg, D.** and **Jucker, M.**, *The Amyloid State of Proteins in Human Diseases*, Cell, 2012.

[6] **Tuomas P. J. Knowles, M. V.** and **Dobson, C. M.**, *The amyloid state and its association with protein misfolding diseases*, Nature reviews molecular cell biology, 2014.

[7] **Sacchettini, J. C.** and **Kelly, J. W.**, *Therapeutic strategies for human amyloid diseases*, Nature Reviews Drug Discovery, 2002.

[8] **Daniel Kaganovich, R. K.** and **Frydman, J.**, *Misfolded proteins partition between two distinct quality control compartments*, Nature, 2008.

[9] **Tyedmers, J., Mogk, A.** and **Bukau, B.**, *Cellular strategies for controlling protein aggregation*, Nat Rev Mol Cell Biol, Vol. 11, No. 11, pp. 777–788, Nov 2010.

[10] **Specht, S., Miller, S. B. M., Mogk, A.** and **Bukau, B.**, *Hsp42 is required for sequestration of protein aggregates into deposition sites in Saccharomyces cerevisiae*, The Journal of Cell Biology, Vol. 195, No. 4, pp. 617–629, Nov 2011.

[11] **Stephanie EscusaToret, W. I. M. V.** and **Frydman, J.**, *Spatial sequestration of misfolded proteins by a dynamic chaperone pathway enhances cellular fitness during stress*, Nature Cell Biology, 2013.

[12] **Malinovska L, Kroschwald S, M. M. R. D. A. S.**, *Molecular chaperones and stress inducible protein sorting factors coordinate the spatiotemporal distribution of protein aggregates*, Molecular biology of the cell, 2012.

[13] **Liu, I., Chiu, S., Lee, H.** and **Leu, J.**, *The histone deacetylase Hos2 forms an Hsp42 dependent cytoplasmic granule in quiescent yeast cells*, Molecular Biology of the Cell, Vol. 23, No. 7, pp. 1231–1242, Apr 2012.

[14] **Lynn E. Horton, Philip James, E. A. C.** and **Hensold, J. O.**, *The yeast hsp70 homologue Ssa is required for translation and interacts with Sis1 and Pab1 on translating ribosomes*, Journal of biological chemistry, 2001.

[15] **Kabani, M.** and **Martineau, C. N.**, *Multiple Hsp70 Isoforms in the Eukaryotic Cytosol: Mere Redundancy or Functional Specificity?*, Current Genomics, 2008.

[16] **Hartl, F. U.** and **Hayer-Hartl, M.**, *Converging concepts of protein folding in vitro and in vivo*, Nature Structural and Molecular Biology 38; Molecular Biology, Vol. 16, No. 6, pp. 574–581, Jun 2009.

[17] **Saibil, H.**, *Chaperone machines for protein folding, unfolding and disaggregation*, Nature reviews molecular cell biology, 2013.

[18] **Juliane Winkler, Jens Tyedmers, B. B.** and **Mogk, A.**, *Chaperone networks in protein disaggregation and prion propagation,*, Journal of Structural Biology, 2012.

[19] **Tobias Haslberger, Jimena Weibezahn, R. Z. S. L. F. T. T. B. B. A. M.**, *M Domains Couple the ClpB Threading Motor with the DnaK Chaperone Activity*, Molecular cell, 2007.

[20] **Fabian Seyffer, Eva Kummer, Y. O. J. W. M. K. R. Z. V. S. B. B.** and **Mogk, A.**, *Hsp70 proteins bind Hsp100 regulatory M domains to activate AAA disaggregase at aggregate surfaces*, Nature structural and molecular biology, 2012.

[21] **Yuki Oguchi, Eva Kummer, F. S. M. B. B. A. R. Z. R. C. W. A. M.** and **Bukau, B.**, *A tightly regulated molecular toggle controls AAA+ disaggregase*, Nature structural and molecular biology, 2012.

[22] **Shannon M. Doyle, O. G.** and **Wickner, S.**, *Protein rescue from aggregates by powerful molecular chaperone machines*, Nature reviews molecular cell biology, 2013.

[23] **Valeria Cherkasov, Sarah Hofmann, S. D. A. A. M. J. T. G. S. B. B.**, *Coordination of Translational Control and Protein Homeostasis during Severe Heat Stress*, Current biology, 2013.

[24] **Marta del Alamo, Daniel J. Hogan, S. P. V. A. P. O. B. J. F.**, *Defining the Specificity of Cotranslationally Acting Chaperones by Systematic Analysis of mRNAs Associated with Ribosome Nascent Chain Complexes*, PLOS Biology, 2011.

[25] **Veronique Albanese, S. R.** and **Frydman, J.**, *A ribosome anchored chaperone network that facilitates eukaryotic ribosome biogenesis*, Journal of cell biology, 2010.

[26] **Koplin, A., Preissler, S., Ilina, Y., Koch, M., Scior, A., Erhardt, M.** and **Deuerling, E.**, *A dual function for chaperones SSB-RAC and the NAC nascent polypeptide-associated complex on ribosomes*, The Journal of Cell Biology, Vol. 189, No. 1, pp. 57–68, Apr 2010.

[27] **Kramer, G., Boehringer, D., Ban, N.** and **Bukau, B.**, *The ribosome as a platform for co-translational processing, folding and targeting of newly synthesized proteins*, Nature Structural and Molecular Biology38; Molecular Biology, Vol. 16, No. 6, pp. 589–597, Jun 2009.

[28] **Peggy Huang, Matthias Gautschi, W. W. S. R.** and **Craig, E. A.**, *The Hsp70 Ssz1 modulates the function of the ribosome associated J protein Zuo1*, Nature Structural & Molecular Biology, 2005.

[29] **Kristin Peisker, Daniel Braun, T. W. J. H. U. F. G. F. A. S.** and **Rospert, S.**, *Ribosome associated Complex Binds to Ribosomes in Close Proximity of Rpl31 at the Exit of the Polypeptide Tunnel in Yeast*, Molecular Biology of the Cell, 2008.

[30] **Kristin Peiskera, Marco Chiabudinib, S. R.**, *The ribosome-bound Hsp70 homolog Ssb of Saccharomyces cerevisiae*, Biochimica et Biophysica Acta (BBA) - Molecular Cell Research, 2010.

[31] **Preissler, S.** and **Deuerling, E.**, *Ribosome-associated chaperones as key players in proteostasis*, Trends in Biochemical Sciences, 2012.

[32] **Felix Willmund, Marta del Alamo, S. P. T. C. V. A. E. B. D. J. P.** and **Frydman, J.**, *The cotranslational function of ribosome associated Hsp70 in eukaryotic protein homeostasis*, Cell, 2013.

[33] **Charlotte Conz, Hendrik Otto, K. P. M. G. T. W. M. P. M.** and **Rospert, S.**, *Functional Characterization of the Atypical Hsp70 Subunit of Yeast Ribosome associated Complex*, Journal of Biological Chemistry, 2007.

[34] **Matthias Gautschi, Hauke Lilie, U. F. A. M. S. R. T. L. P. R.** and **Rospert, S.**, *RAC a stable ribosome associated complex in yeast formed by the DnaK DnaJ homologs Ssz1p and zuotin*, Proceedings of National Academy of Sciences, 2001.

[35] **Zdravko Dragovic, Yasuhito Shomura, N. T. F. U. H.** and **Bracher, A.**, *Fes1p acts as a nucleotide exchange factor for the ribosome associated molecular chaperone Ssb1p*, Biological Chemistry, 2006.

[36] **Holger Raviol, Heather Sadlish, F. R. M. P. M.** and **Bukau, B.**, *Chaperone network in the yeast cytosol Hsp110 is revealed as an Hsp70 nucleotide exchange factor*, EMBO Journal, 2006.

[37] **Holger Sondermann, Albert K. Ho, L. L. L. K. S. I. M. S. R. W. F.-U. H.** and **Young, J. C.**, *Prediction of novel Bag1 homologs based on structure function analysis identifies Snl1p as an Hsp70 cochaperone in Saccharomyces cerevisiae*, Journal of biological chemistry, 2002.

[38] **Alice Yen-Wen Yam, Veronique Albanese, H.-T. J. L.** and **Frydman, J.**, *Hsp110 cooperates with different cytosolic HSP70 systems in a pathway for de novo folding*, Journal of biological chemistry, 2005.

[39] **Matthias Gautschi, Andrej Mun, S. R.** and **Rospert, S.**, *A functional chaperone triad on the yeast ribosome*, Proceedings of National Academy of Sciences, 2002.

[40] **Wei Yan, Brenda Schilke, C. P. W. W. S. K.** and **A.Craig, E.**, *Zuotin a ribosome associated DnaJ molecular chaperone*, EMBO Journal, 1998.

[41] **Veronique Albanese, Alice Yen Wen Yam, J. B. C. P. J. F.**, *Systems analyses reveal two chaperone networks with distinct functions in eukaryotic cells*, Cell, 2006.

[42] **R.John Nelson, Thomas Ziegelhoffer, C. N. M. W. W.** and **Craig, E. A.**, *The translation machinery and 70 kDa heat shock protein cooperate in protein synthesis*, Cell, 1992.

[43] **Christine Pfund, Nelson Lopez Hoyo, T. Z. B. A. S. P. L. B. W. A. W.-M. W.** and **Craig, E. A.**, *The molecular chaperone Ssb from Saccharomyces cerevisiae is a component of the ribosome nascent chain complex*, EMBO Journal, 1998.

[44] **von Plehwe, U., B. U. C. C. C. M. F. E. S. A. P. A. P.-D.** and **S, R.**, *The Hsp70 homolog Ssb is essential for glucose sensing via the SNF1 kinase network*, Genes & Development, Vol. 23, No. 17, pp. 2102–2115, Sep 2009.

[45] **Finley, D.**, *Recognition and Processing of Ubiquitin-Protein Conjugates by the Proteasome*, Annual reviews of Biochemistry, 2009.

[46] **Maria A. Theodoraki, Nadinath B. Nillegoda, J. S.** and **Caplan, A. J.**, *A network of ubiquitin ligases is important for the dynamics of misfolded protein aggregates in yeast*, Journal of biological chemistry, 2012.

[47] **Hilla Weidberg, E. S.** and **Elazar, Z.**, *Biogenesis and Cargo Selectivity of Autophagosomes*, The Annual Review of Biochemistry, 2011.

[48] **Kefeng Lu, Ivan Psakhye, S. J.**, *Autophagic Clearance of PolyQ Proteins Mediated by Ubiquitin-Atg8 Adaptors of the Conserved CUET Protein Family*, Cell, 2014.

[49] **Breker, M., Gymrek, M.** and **Schuldiner, M.**, *A novel single-cell screening platform reveals proteome plasticity during yeast stress responses*, The Journal of Cell Biology, Vol. 200, No. 6, pp. 839–850, Mar 2013.

[50] **An, S., Kumar, R., Sheets, E. D.** and **Benkovic, S. J.**, *Reversible Compartmentalization of de Novo Purine Biosynthetic Complexes in Living Cells*, Science, Vol. 320, No. 5872, pp. 103–106, Apr 2008.

[51] **Laporte, D., Salin, B., Daignan-Fornier, B.** and **Sagot, I.**, *Reversible cytoplasmic localization of the proteasome in quiescent yeast cells*, The Journal of Cell Biology, Vol. 181, No. 5, pp. 737–745, May 2008.

[52] **Noree, C., Sato, B. K., Broyer, R. M.** and **Wilhelm, J. E.**, *Identification of novel filament-forming proteins in Saccharomyces cerevisiae and Drosophila melanogaster*, The Journal of Cell Biology, Vol. 190, No. 4, pp. 541–551, Aug 2010.

[53] **Narayanaswamy, R., Levy, M., Tsechansky, M., Stovall, G. M., O'Connell, J. D., Mirrielees, J., Ellington, A. D.** and **Marcotte, E. M.**, *Widespread reorganization of metabolic enzymes into reversible assemblies upon nutrient starvation*, Proceedings of the National Academy of Sciences, 2009.

[54] **Bodies, A., in Yeast, Cells, Q., Immediately, A.** and **Reserve?, A. A.**, *Molecular Biology of the Cell Vol. 17, 4645Đ4655, November*, 2006.

[55] **Laporte, D., Lebaudy, A., Sahin, A., Pinson, B., Ceschin, J., Daignan-Fornier, B.** and **Sagot, I.**, *Metabolic status rather than cell cycle signals control quiescence entry and exit*, The Journal of Cell Biology, Vol. 192, No. 6, pp. 949–957, Mar 2011.

[56] **EMBO** and **NAL, J.**, *The EMBO Journal*, 2011.

[57] **Rambold, A. S., Kostelecky, B., Elia, N.** and **Lippincott-Schwartz, J.**, *Tubular network formation protects mitochondria from autophagosomal degradation during nutrient starvation*, Proceedings of the National Academy of Sciences, Vol. 108, No. 25, pp. 10190–10195, Jun 2011.

[58] **Pilong Li, Sudeep Banjade, H.-C. C. S. K. B. C. L. G. M. L. J. V. H. D. S. K. S. F. B. P. S. R. Q.-X. J. B. T. N.** and **Rosen, M. K.**, *Phase Transitions in the Assembly of Multi-Valent Signaling Proteins*, Nature, 2012.

[59] **OâConnell, J. D., Tsechansky, M., Royall, A., Boutz, D. R., Ellington, A. D.** and **Marcotte, E. M.**, *A proteomic survey of widespread protein aggregation in yeast*, Mol. BioSyst., Vol. 10, No. 4, pp. 851, 2014.

[60] **Zaman, S., Lippman, S. I., Zhao, X.** and **Broach, J. R.**, *How Saccharomyces Responds to Nutrients*, Annual Review of Genetics, Vol. 42, No. 1, pp. 27–81, Dec 2008.

[61] **Jacinto, E.** and **N.Hall, M.**, *TOR signalling in bugs, brain and brawn*, Nature reviews molecular cell biology, 2003.

[62] **Nair, U., Jotwani, A., Geng, J., Gammoh, N., Richerson, D., Yen, W.-L., Griffith, J., Nag, S., Wang, K., Moss, T.** and **et al.**, *SNARE Proteins Are Required for Macroautophagy*, Cell, Vol. 146, No. 2, pp. 290–302, Jul 2011.

[63] **Hirohito Haruki, J. N.** and **Laemmli, U. K.**, *The Anchor away Technique. Rapid, Conditional Establishment of Yeast Mutant Phenotypes*, Molecular Cell, Vol. 31, No. 6, pp. 925– 932, Sep 2008.

[64] **Voss, C., Lahiri, S., Young, B. P., Loewen, C. J.** and **Prinz, W. A.**, *ER-shaping proteins facilitate lipid exchange between the ER and mitochondria in S. cerevisiae*, Journal of Cell Science, Vol. 125, No. 20, pp. 4791–4799, Oct 2012.

[65] **Jacquier, N., Choudhary, V., Mari, M., Toulmay, A., Reggiori, F.** and **Schneiter, R.**, *Lipid droplets are functionally connected to the endoplasmic reticulum in Saccharomyces cerevisiae*, Journal of Cell Science, Vol. 124, No. 14, pp. 2424–2437, Jul 2011.

[66] **Laporte, D., Courtout, F., Salin, B., Ceschin, J.** and **Sagot, I.**, *An array of nuclear microtubules reorganizes the budding yeast nucleus during quiescence*, The Journal of Cell Biology, Vol. 203, No. 4, pp. 585–594, Nov 2013.

[67] **Zhao, A., Tsechansky, M., Swaminathan, J., Cook, L., Ellington, A. D.** and **Marcotte, E. M.**, *Transiently Transfected Purine Biosynthetic Enzymes Form Stress Bodies*, PLoS ONE, Vol. 8, No. 2, pp. 56203, Feb 2013.

[68] **Cabiscol, E.**, *Oxidative stress promotes specific protein damage in Saccharomyces cerevisiae*, Journal of Biological Chemistry, Jun 2000.

[69] **Tyedmers, J., Treusch, S., Dong, J., McCaffery, J. M., Bevis, B.** and **Lindquist, S.**, *Prion induction involves an ancient system for the sequestration of aggregated proteins and heritable changes in prion fragmentation*, Proceedings of the National Academy of Sciences, Vol. 107, No. 19, pp. 8633–8638, May 2010.

[70] **Ivana Petrovska, Elisabeth Nuske, M. C. M. G. K. L. M. S. K. D. R. K. F. K. G. J. M. V. S. A.**, *Filament formation by metabolic enzymes is a specific adaptation to an advanced state of cellular starvation*, Elife, 2014.

[71] **Peters, L. Z., Hazan, R., Breker, M., Schuldiner, M.** and **Ben-Aroya, S.**, *Formation and dissociation of proteasome storage granules are regulated by cytosolic pH*, The Journal of Cell Biology, Vol. 201, No. 5, pp. 663–671, May 2013.

[72] **Thibault, G., Shui, G., Kim, W., McAlister, G., Ismail, N., Gygi, S., Wenk, M.** and **Ng, D.**, *The Membrane Stress Response Buffers Lethal Effects of Lipid Disequilibrium by Reprogramming the Protein Homeostasis Network*, Molecular Cell, Vol. 48, No. 1, pp. 16–27, Oct 2012.